

Curvature of the spectral energy distribution, the dominant process for inverse Compton component and other jet properties in Fermi 2LAC blazars

R. Xue¹, D. Luo¹, L. M. Du^{1*}, Z. R. Wang¹, Z. H. Xie¹, T. F. Yi¹, D. R. Xiong², Y. B. Xu¹, W. G. Liu¹ and X. L. Yu¹

¹*Department of Physics, Yunnan Normal University, Kunming 650500, China*

²*National Astronomical Observatories/Yunnan Observatories, Chinese Academy of Sciences, Kunming 650011, China*

20 September 2016

ABSTRACT

We fit the spectral energy distributions (SEDs) of members of a large sample of Fermi 2LAC blazars to synchrotron and inverse Compton (IC) models. Our main results are as follows. (i) As suggested by previous works, the correlation between peak frequency and curvature can be explained by statistical or stochastic particle acceleration mechanisms. For BL Lacs, we find a linear correlation between synchrotron peak frequency and its curvature. The slope of the correlation is consistent with the stochastic acceleration mechanisms and confirm previous studies. For FSRQs, we also find a linear correlation, but its slope cannot be explained by previous theoretical models. (ii) We find a significant correlation between IC luminosity and synchrotron luminosity. The slope of the correlation of FSRQs is consistent with the EC process. And the slope of the correlation of BL Lac is consistent with the SSC process. (iii) We find several significant correlations between IC curvature and several basic parameters of blazars (black hole mass, broad line luminosity, the Lorentz factor of jet). We also find significant correlations between bolometric luminosity and these basic parameters of blazars which suggest that the origin of jet is a mixture of the mechanisms proposed by Blandford & Znajek and by Blandford & Payne.

Key words: radiation mechanisms: nonthermal – galaxies: active – galaxies: jet – BL Lacertae objects: general

1 INTRODUCTION

Blazars are the most extreme form of active galactic nuclei (AGN), with their jets pointed in the direction of the observer (Urry & Padovani 1995). The typical spectral energy distribution (SED) of blazars is generally described by a double bump structure. Harvey, Wilking & Joy (1982) were the first to propose using a smooth spectrum instead of a segmented power-law spectrum when they researched the submillimeter band of 3C 345. Landau (1983) researched a sample in the centimeter, millimeter and optical bands that consisted of 9 quasi-stellar objects (QSOs) and BL Lacs. Landau et al. (1986) analyzed a sample of low-energy peaked BL Lac objects from the millimeter band to the ultraviolet band, and found that, although they could obtain spectrum successfully when combined with power-law spectrum, the data from the radio to the ultraviolet band showed good consis-

tency with the smooth spectrum many cases. They used a quadratic function, namely:

$$\log S_\nu = C + [(\log \nu - B)^2] / 2A \quad (1)$$

to fit the spectrum. Massaro et al. (2004a) found that the log-parabolic law can well describe the X-ray peak value of SED of Mrk 421, and subsequent found that log-parabolic law can fit the X-ray spectrum (Massaro et al. 2008).

There is, however, a problem in using the log-parabolic law to fit SEDs: some parameters in the equation do not have a physical explanation. It is remarkable that the SEDs of many sources can be fitted by a quadratic function that contains three parameters. The property indicates that these sources may have a similar structure, or similar relativistic particle energy distributions, or both (Landau et al. 1986). With a more general and simple situation about the particles increasing their energy, the log-parabolic law is used to statistical acceleration structure. One advantage of log-parabolic law is that it can be used to calculate various

* E-mail: leiming_du@ynao.ac.cn

useful parameters, such as peak frequency, curvature and so on, which is simpler than the case for other models.

When we obtain the value of peak frequency and peak luminosity of SEDs, the curvature of the SEDs will be another important parameter. The curvature is the property possessed by the curving of a line. If the peak frequency and peak luminosity are known, the curvature can be used to derive the bolometric luminosity. The relationship between the peak frequency and the curvature can be explained in terms of the acceleration process of emitting electrons (Massaro et al. 2004a, 2004b, 2006; Paggi et al. 2009a, 2009b; Rani et al. 2011; Tramacere et al. 2007, 2009, 2011; Chen 2014). Chen (2014) performed an analysis of the curvature-peak frequency connection, and re-derived a theoretical model that some authors had used before (Massaro et al. 2004a, 2006; Tramacere et al. 2011). He predicted two electron acceleration mechanisms according to the coefficient of the curvature-peak frequency relationship. For models of stochastic acceleration, the values of the energy-dependent acceleration probability, the fluctuation of the fractional acceleration gain (the latter two are statistical acceleration) and the slope $k(1/c = k\log\nu_p + h)$ are 2, 2.5, 3.333 respectively. The result of Chen (2014) was 2 which is consistent with stochastic acceleration.

The SEDs generated by two emission components, namely the synchrotron component and inverse Compton (IC) component (Ghisellini et al. 1997; Massaro et al. 2004a, 2006). In the lepton model, it is generally accepted that low-energy peak is caused by the synchrotron emission of relativistic electrons in the jet, and that the high energy peak is caused by IC scattering (Massaro et al. 2004, 2006; Meyer et al. 2012). There is, however, disagreement concerning the origin of the soft photons of IC scattering. (1) They are derived from synchrotron emission, termed the synchrotron self-Compton (SSC) process (Rees 1967; Jones et al. 1974; Marscher & Gear 1985; Maraschi et al. 1992; Sikora et al. 1994; Bloom & Marscher 1996). (2) They are derived from the exterior of jets, termed the external Compton (EC) process. There are three possible sources of EC soft photons: accretion disk photons entering jets directly (Dermer et al. 1992; Dermer & Schlickeiser 1993); broad line region (BLR) photons entering jets (Sikora et al. 1994; Dermer et al. 1997); and dust torus infrared radiation photons entering jets (Blazewski et al. 2000; Arbeiter et al. 2002). Ghisellini (1996) derived two relationships between the synchrotron luminosity and the IC luminosity so that it could be determined whether the IC component is dominated by the EC process or the SSC process ($L_{EC} \sim L_{syn}^{1.5}$, $L_{SSC} \sim L_{syn}^{1.0}$).

The bolometric luminosity is one of the most important parameters of blazars. It represents the amount of electromagnetic energy a body radiates per unit of time. Thus it represents the total radiant energy over a wide band (from the radio band to the γ band). In research concerning the origin of jets, the current theoretical model is that the jet power is generated from accretion and the extraction of rotational energy or angular momentum from disc/black hole (Blandford & Znajek 1977; Blandford & Payne 1982). The black hole and accretion disc play an important role in the process, so it is important to research the relationships between the jet and black hole and between the jet and accretion. Ghisellini et al. (2010) found that Fermi blazars with higher luminosities may have a larger black hole. Xiong

et al. (2014a) researched the relationship between the jet power and black hole mass and found that there is a significant correlation between them, which means that the jet power is controlled by the spin of black hole. In both mechanisms, the magnetic field plays a major role in channelling power from the black hole or the disc into the jet. The process be sustained by matter accreting on to black hole, so it is reasonable that there is connection between the origin of jet and accretion (Maraschi & Tavecchio 2003). Many authors have studied the jet-accretion disk relationship, using a variety of methods (Rawlings & Saunders 1991; Falcke & Biermann 1995; Serjeant et al. 1998; Cao & Jiang 1999; Wang et al. 2004; Liu et al. 2006; Xie et al. 2007; Gu et al. 2009; Ghisellini et al. 2009a, 2009b, 2010, 2011; Sbarrato et al. 2012; Yu et al. 2015). The BLR luminosity can be taken as an indicator of the accretion power of blazars (Celotti, Padovani & Ghisellini 1997), and the bolometric luminosity can be taken as the index of jet power, so researching the relationship between the BLR luminosity and bolometric luminosity can provide information on the relationship between the jet and accretion disc, contributing to the knowledge about the origin of jets. Xie et al. (2007) found a significant correlation between $\log L_{BLR}$ and $\log L_{jet}$ ($\log L_{BLR} = \log L_{jet} + \log \eta + \text{const}$). The Lorentz factor (Γ) can describe the speed of the jet flow (Hovatta et al. 2009). There is a relationship between the jet power and jet speed: more powerful jets will appear to be faster (Kharb et al. 2010). Lü et al. (2012) found that the Γ and γ -luminosity are significant connection. We know that the γ -luminosity can represent the bolometric luminosity (Fan, Xie, & Bacon 1999, Xie et al. 2004), so we can predict that there will be a linear correlation between Γ and bolometric luminosity.

In this paper, the SEDs of both synchrotron and IC components of a sample are fitted by a log-parabolic law. The bolometric luminosity is the amount of electromagnetic energy a body radiates per unit of time, it is the total radiant energy over a wide band (from the radio band to the γ band), we calculate the exact value of the bolometric luminosity and curvature by fitting the SEDs. Firstly, we analyse the curvature-peak frequency relation and try to verify the particle acceleration mechanism. Then, we analyse the correlation between the IC luminosity and the synchrotron luminosity and try to judge the IC component is dominated by the EC process or the SSC process. Finally, we analyse the correlations between curvature, bolometric luminosity and black hole mass, BLR luminosity and the Lorentz factor.

The paper is structured as follows. In Section 2 we present the sample; In Section 3 we detail the fitting procedure; in Section 4, we present the results; In Section 5 we provide a discussion and conclusion. A Λ CDM cosmology with $H_0 = 70 \text{ Kms}^{-1} \text{ Mpc}^{-1}$, $\Omega_m = 0.27$, $\Omega_\Lambda = 0.73$ is adopted.

2 THE SAMPLE

We collected a sample from the second LAT AGN catalog (2LAC). At least one of the two components (synchrotron and IC component) of the blazars in our sample can be fitted by sufficient multifrequency data coverage. The sample contains 279 blazars, including 200 flat-spectrum radio quasars (FSRQs) and 79 BL Lacs. For the FSRQs, the

IC components of 98 objects and the synchrotron components of 21 FSRQs cannot be fitted, while the complete SEDs of 81 FSRQs can be fitted. For the BL Lacs, the IC components of 46 objects and the synchrotron components of 5 objects cannot be fitted, while the complete SEDs of 28 BL Lacs can be fitted. According to Abdo et al. 2010, blazars can be subdivided into three subclasses, namely LSP(low synchrotron-peaked, $\nu_{peak}^{syn} < 10^{14}$ Hz), ISP(intermediate synchrotron-peaked, $10^{14}Hz < \nu_{peak}^{syn} < 10^{15}$ Hz) and HSP(high synchrotron-peaked, $\nu_{peak}^{syn} > 10^{15}$ Hz). For FSRQs, 179 (89.5 percent of the total) have an SED classification, namely 175 LSPs and 4 ISPs. For BL Lacs, 74(93.7 percent of the total) have an SED classification, namely 37 LSPs, 11 ISPs and 26 HSPs.

For our sample, biases are as follows:

(1) For blazars in 2LAC, 526 had an SED classification, with LSP representing the largest subclass(282/526=54 percent)(Ackermann et al. 2011). Our sample is a subsample of 2LAC, and 83.8 percent(212/253=83.8 percent) are LSPs. Compared with 2LAC, our sample is more dominated by LSPs.

(2) Fermi data were integrated over a few months(Abdo et al. 2010, Giommi et al. 2012a), and therefore the SED fitting, luminosity calculation and correlation analysis concerning the γ -ray band in this paper cannot be considered simultaneous in this paper. However, at least the fitting of synchrotron component can be considered simultaneous. The observation date of the (quasi-) simultaneous data of blazars whose IC components can be fitted is in the period of the Fermi exposure time.

(3) Redshift can be measured with a clear spectrum. However, BL Lacs typically lack some emission lines, so the redshift will not be accurate. This lack can affect the rest-frame correction, the luminosity calculation and the related correlation analysis(a detailed discussion is given in Sect. 5.1).

Detailed information about the sample is given in Table 5, with the following headings: column (1), name of Fermi catalog; column (2), redshift; column (3), the observation date of the (quasi-)simultaneous data; column (4), logarithm of the synchrotron peak frequency in units of Hz; column (5), second degree term of log-parabolic for the synchrotron component and the IC component; column (6), logarithm of the black hole mass in the unit of M_{\odot} ; column (7), logarithm of the broad-line luminosity in the units of erg s^{-1} ; column (8), Lorentz factor of jet; column (9), logarithm of luminosity for the synchrotron component and IC component in the units of erg s^{-1} ; column (10), logarithm of the bolometric luminosity in the units of erg s^{-1} ; column (11), type of the blazar.

For BL Lacs without a measured redshift, we assume the mean redshift value of 0.27 in 2LAC(Ackermann et al. 2011). For the 95 blazars for which more than one black hole masses is given in the literature, we use the average black hole mass instead in the related correlation analysis. All the values of luminosity are integrated from the SEDs.

3 THE FITTING PROCEDURE

We construct the SEDs of all the blazars in our samples from the multifrequency data using the ASDC SED Builder,

an online service developed at the ASI Science Data Center(Stratta et al. 2011). We use the second-degree polynomial function

$$\log(\nu F_{\nu}) = c(\log\nu)^2 + b(\log\nu) + a \quad (2)$$

to fit the synchrotron component and IC component separately, so that we could calculate the curvature around the peak(where the curvature is represented by $|2c|$). In this paper, all values are converted into the rest-frame. The parameters in the rest-frame of the second-degree polynomial function and the peak frequency can be calculated as:

$$a_{rest} = a - b\Delta + c\Delta^2 + \log 4\pi + 2\log D_L \quad (3)$$

$$b_{rest} = b - 2c\Delta \quad (4)$$

$$c_{rest} = c \quad (5)$$

$$\nu_{p,rest} = \nu_p^{obs}(1+z) \quad (6)$$

, where D_L is the luminosity distance, z is the source redshift and $\Delta = \log(1+z)$. The database of the ASDC SED Builder provides the observational data from many space telescopes and ground-based telescopes, and we can obtain simultaneous data based on the observation times provided. The IC components of some blazars(e.g. BL Lac-HSPs) covered only the γ -ray band, and therefore the IC-fitted parameters may be unreliable because of the narrow data coverage. In these cases we did not provide fits. According to the synchrotron and IC fitting curves, we can calculate the bolometric flux as follows:

$$F_{integrated} = \int F_{\nu} d\nu = (\ln 10) \int 10^{(cx^2 + bx + a)} dx \quad (7)$$

The bolometric luminosity can be calculated using the relationship:

$$L_{bol} = 4\pi D_L^2 F_{integrated}. \quad (8)$$

The biases and uncertainties that might be caused by the above procedure are as follows:

1. The thermal radiation from the disc/torus and the host galaxy is prominent in both the optical/IR and the UV wavebands(Ackermann et al. 2015, Giommi et al. 2012a, Abdo et al. 2010, Marscher 2009). Before fitting the SED, we had to exclude the thermal radiation because it will amplify the emission from the jets of blazars. We identified the thermal component by visual inspection, so we can separate the radiation whose flux is significantly greater than the non-thermal radiation at ultraviolet frequencies.

2. In this paper, the SEDs are fitted using a second-degree polynomial. However, the second-degree polynomial cannot handle asymmetry very well and may skew some relevant results(for example in the luminosity calculation). In order to evaluate this effect, we used four typical BL Lacs with an apparent asymmetrical synchrotron component, namely 2FGLJ0050.6-0929, 2FGLJ0136.5+3905, 2FGLJ1015.1+4925 and 2FGLJ1136.7+7009, and fitted their synchrotron component with a second-degree polynomial and with a third-degree polynomial and then compare the synchrotron luminosities. For the second-degree polynomial, the logarithms of synchrotron luminosity were 47.2, 46.8, 46.1 and 44.6. For the third-degree polynomial, the synchrotron luminosities were 46.6, 46.1, 45.2 and 44.0. From the above results, we found that the logarithm of synchrotron luminosity integrated by the third-degree polynomial is lower

than that from the second-degree polynomial, and the numerical differences are within 1. We therefore suggest that the impact on calculation of luminosity is insignificant, and will not affect the main results in this paper.

3. The light variability of blazars can cause massive changes in the SED curve, peak frequency, peak flux, curvature, etc (Massaro et al. 2004a, Massaro et al. 2004b, Acciari et al. 2011). In this paper, we make sure that the fitted data were observed contemporaneously. The influence of light variability is not considered here. In order to make use of the maximum availability of (quasi-)simultaneous data coverage, SEDs in both low and high states are considered. This might contribute to the scatter in the correlation analysis below

4 THE RESULTS

Three sub-samples selected from our sample were analysed using linear correlations. The sub-samples are as follows:

(A) FSRQs ($N=179$, where N is number of objects in the sample) and BL Lacs ($N=74$) with fitted synchrotron components. We studied the correlation between synchrotron peak frequency and its curvature using this subsample.

(B) FSRQs ($N=81$) and BL Lacs ($N=28$) with fitted complete SEDs. We studied the correlation between the IC luminosity and synchrotron luminosity using this subsample.

(C) FSRQs ($N=59$) with black hole masses, broad line luminosity, Lorentz factor and fitted complete SEDs. This is a clean sample for FSRQs. For the three subsamples, biases are as follows:

(1) We used sub-samples A and B for the following reasons. First, they enable the study of interesting correlations that are important for FSRQs and BL Lacs. Second, the statistical significance is maximized because they provide the maximum availability of data. As noted above, these two subsamples predominantly contain objects with low peaks. This means that they might give biased results. The subsamples could give more reliable results if they contained more high-peaked BL Lacs. Fortunately, although the redshifts of BL Lacs are not measured accurately, these two correlations are not affected seriously.

(2) Only 59 FSRQs ($59/281=21$ percent) get a complete SED and data for the black hole mass, broad-line luminosity and Lorentz factor. The rest of the sample do not have all the data (black hole mass, broad-line luminosity or the Lorentz factor) or a complete SEDs. The missing data may have an enormous impact on the correlation analysis, and it is difficult to assess what has happened to the sample between each plots. Therefore, the results that we obtain are only for our subsample. A larger clean sample of FSRQs is needed to check these results in detail.

4.1 Synchrotron peak frequency vs synchrotron curvature in FSRQs and BL Lacs

The synchrotron peak frequency versus synchrotron curvature is plotted in Fig. 1 using data from subsample A.. Here we use the $-1/c_{syn}$ instead of $2(-c_{syn})$ to represent the synchrotron curvature because it will be convenient to compare with the theoretical results (see Chen

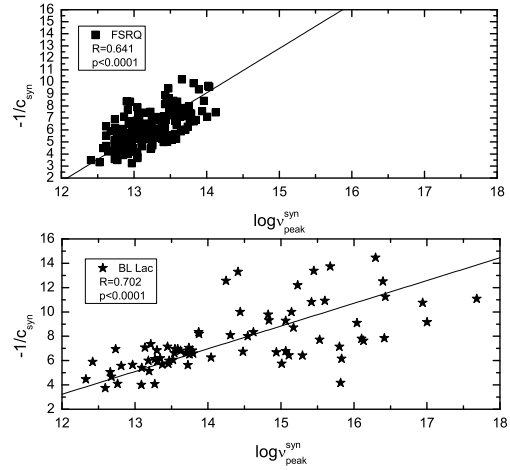


Figure 1. Top panel: The correlation between $\log \nu_{peak}^{syn}$ and $-1/c_{syn}$ for FSRQs. The solid line is the best linear fitting ($p < 0.0001$). Bottom panel: The correlation between $\log \nu_{peak}^{syn}$ and $-1/c_{syn}$ for BL Lacs. The solid line is the best linear fitting ($p < 0.0001$).

2014). The Spearman test was used to analyse the correlation between $\log \nu_{peak}^{syn}$ and $-1/c_{syn}$ for FSRQs (top panel) and BL Lacs (bottom panel). We assume that the correlation is significant when $p < 0.05$. For FSRQs, the Spearman test gives a significance level $p < 0.0001$ and a coefficient of correlation $R=0.641$. The bisector linear regression gives the best linear fitting equation as $-1/c_{syn} = (3.69 \pm 0.24) \log \nu_{peak}^{syn} + (-42.57 \pm 3.14)$. For BL Lacs, the Spearman test gives a significance level $p < 0.0001$ and a coefficient of correlation $R=0.702$. The bisector linear regression gives the best linear fitting equation as $-1/c_{syn} = (1.87 \pm 0.19) \log \nu_{peak}^{syn} + (-19.21 \pm 2.76)$. The results show that the correlations between $\log \nu_{peak}^{syn}$ and $-1/c_{syn}$ for FSRQs and BL Lacs are significant. For BL Lacs, the slope of the correlation ($k_{BL Lac} = 1.87 \pm 0.19$) is consistent with the stochastic acceleration mechanism (Chen 2014). For FSRQs, however, the slope ($k_{FSRQ} = 3.69 \pm 0.24$) is not consistent with any of the theoretical values provided by Chen (2014). The distribution (the bottom panel of Fig. 1) of BL Lac-ISP and BL Lac-HSPs is more dispersed than the distribution of BL Lacs-LSPs. If the number of BL Lac-ISP and BL Lac-HSPs were greatly increased, this may change the slope of the best fit and the significant level.

4.2 Inverse Compton luminosity vs synchrotron luminosity in FSRQs and BL Lacs

The inverse Compton luminosity versus synchrotron luminosity is plotted in Fig. 2 using data from subsample B. The Spearman test was applied in order to analyse the correlation between $\log L_{IC}$ and $\log L_{syn}$ for FSRQs (top panel) and BL Lacs (bottom panel). For FSRQs, the Spearman test gives a significance level $p < 0.0001$ and a coefficient of correlation $R=0.74$. The bisector linear regression gives the best linear fitting equation as $\log L_{IC} = (1.45 \pm 0.11) \log L_{syn} + (-20.10 \pm 5.12)$. For BL Lacs, the Spearman test gives a significance level $p < 0.0001$ and a coefficient of correlation $R=0.901$. The bisector linear regression gives the best

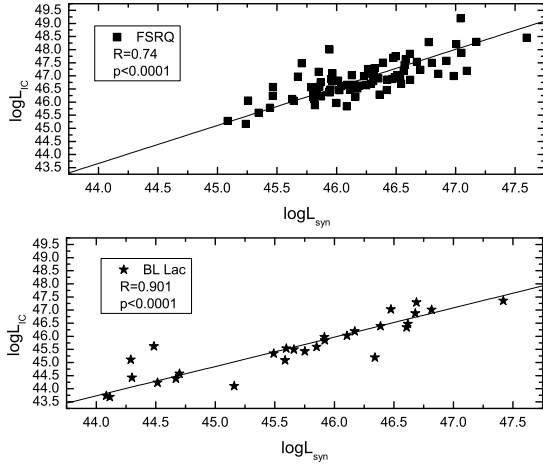


Figure 2. Top panel: The correlation between $\log L_{IC}$ and $\log L_{syn}$ for FSRQs. The solid line is the best linear fitting ($p < 0.0001$). Bottom panel: The correlation between $\log L_{IC}$ and $\log L_{syn}$ for BL Lacs. The solid line is the best linear fitting ($p < 0.0001$).

linear fitting equation as $\log L_{IC} = (1.12 \pm 0.10) \log L_{syn} + (-5.43 \pm 4.61)$. The results show that the correlations between $\log L_{IC}$ and $\log L_{syn}$ for FSRQs and BL Lacs are significant, and $k_{FSRQ} = 1.45 \pm 0.11$, $k_{BLLac} = 1.12 \pm 0.10$. According to Ghisellini (1996) ($L_{EC} \sim L_{syn}^{1.5}$, $L_{SSC} \sim L_{syn}^{1.0}$), our results suggest that the IC component of FSRQs is dominated by the EC process (Ghisellini et al. 2002; Celotti & Ghisellini 2008; Ghisellini et al. 2010; Finke 2013) and that in BL Lacs it is dominated by the SSC process (Zhang et al. 2013; Lister et al. 2011; Celotti & Ghisellini 2008; Ghisellini et al. 2002; Ghisellini et al. 2010; Ackermann et al. 2012). In subsample B, the number of BL Lacs is much lower than the number of FSRQs, and a larger sample of BL Lacs with complete SEDs is needed for further study.

4.3 Broad line luminosity, black hole mass, the Lorentz factor and bolometric luminosity vs curvature in FSRQs

The broad-line luminosity, black hole mass, Lorentz factor and bolometric luminosity are plotted versus IC curvature in Figs 3 to 6 using data from subsample C. It can be seen in these figures that 2FGL J1539.5+2747 and 2FGL J2211.9+2355 could be outliers because of their excessive IC curvature. We checked their fitted SEDs by eye so that fitting errors can be excluded. We also found that the Lorentz factor of 2FGL J1733.1-1307 ($\Gamma = 65.24$) is extremely high. According to Hovatta et al. (2009), either the Lorentz factor is accurate, or the source exhibits so rapid flares that the fast variations were undetected in the monitoring programmes. For this reason, we exclude 2FGL J1733.1-1307 in the following analysis concerning the Lorentz factor, as did Hovatta et al. (2009).

The Spearman test was applied in order to analyse the correlations between the broad-line luminosity, black hole mass, Lorentz factor, bolometric luminosity and IC curvature for FSRQs (there are no correlations between syn-

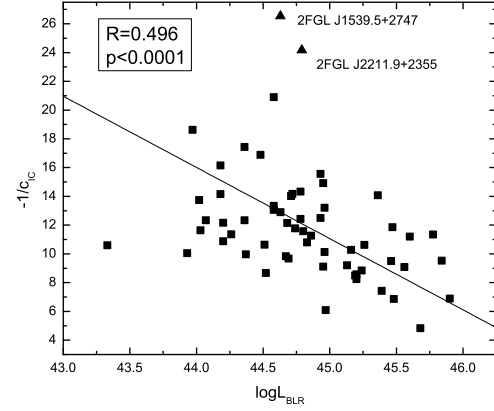


Figure 3. The correlation between $\log L_{BLR}$ and $-1/c_{IC}$ for FSRQs. The solid line is the best linear fitting ($p < 0.0001$).

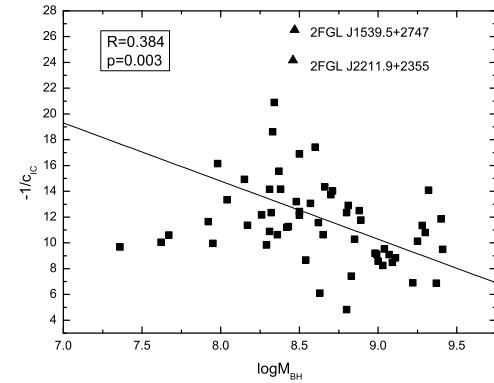


Figure 4. The correlation between $\log M_{BH}$ and $-1/c_{IC}$ for FSRQs. The solid line is the best linear fitting ($p = 0.003$).

chrotron curvature and all the parameters). The results are as follows:

1. $\log L_{BLR}$ vs. $-1/c_{IC}$: $p < 0.0001$, $R = 0.496$.
2. $\log M_{BH}$ vs. $-1/c_{IC}$: $p = 0.003$, $R = 0.384$.
3. Γ vs. $-1/c_{IC}$: $p = 0.001$, $R = 0.418$.
4. $\log L_{bol}$ vs. $-1/c_{IC}$: $p = 0.001$, $R = 0.417$.

The results show that the correlations between all the parameters and the IC curvature for FSRQs are moderately significant. The significant correlation between $\log L_{BLR}$ and $-1/c_{IC}$ can be explained as the origin of the soft photons of the IC component may be dominated by the broad-line region.

4.4 Broad line luminosity, black hole mass and the Lorentz factor vs bolometric luminosity in FSRQs

The broad-line luminosity, black hole mass, and Lorentz factor are plotted versus bolometric luminosity in Figs 7 to 9 using data from subsample C. As noted above, the Lorentz factor of 2FGL J1733.1-1307 is excluded as an outlier. The

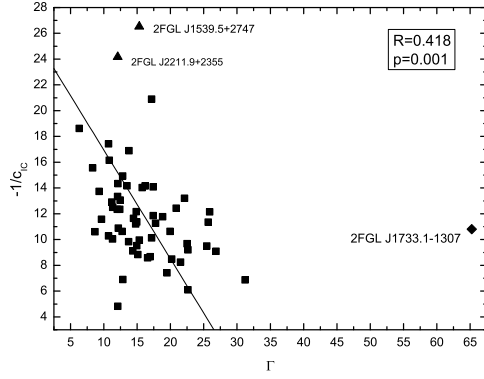


Figure 5. The correlation between Γ and $-1/c_{IC}$ for FSRQs. The solid line is the best linear fitting ($p = 0.001$).

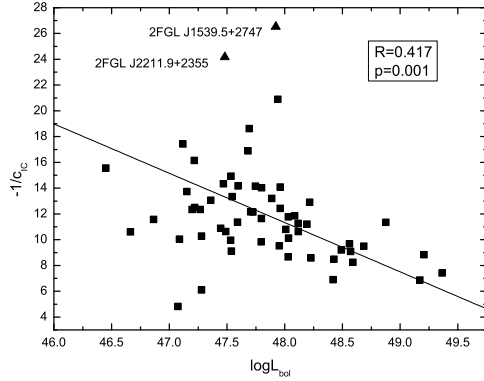


Figure 6. The correlation between $\log L_{bol}$ and $-1/c_{IC}$ for FSRQs. The solid line is the best linear fitting ($p = 0.001$).

Spearman test was applied in order to analyse the correlations between the broad line luminosity, black hole mass, Lorentz factor and bolometric luminosity for FSRQs. The results are as follows:

1. $\log L_{BLR}$ vs. $\log L_{bol}$: $p < 0.0001$, $R=0.575$
2. $\log M_{BH}$ vs. $\log L_{bol}$: $p < 0.0001$, $R=0.47$
3. Γ vs. $\log L_{bol}$: $p < 0.0001$, $R=0.767$

The results show that the correlations between all the parameters and $\log L_{bol}$ for FSRQs are significant. The fact that the correlations between $\log L_{BLR}$, $\log M_{BH}$ and $\log L_{bol}$ are significant support the theory that the origin of jet is a mixture of the mechanisms proposed by Blandford & Znajek and by Blandford & Payne (Punsly & Coroniti 1990; Meier et al. 1999, 2001). Furthermore, the significant correlation between Γ and $\log L_{bol}$ means that more powerful jets, the plasma blob in jets will move faster (Kharb et al. 2010; Wu et al. 2011; Lü et al. 2012).

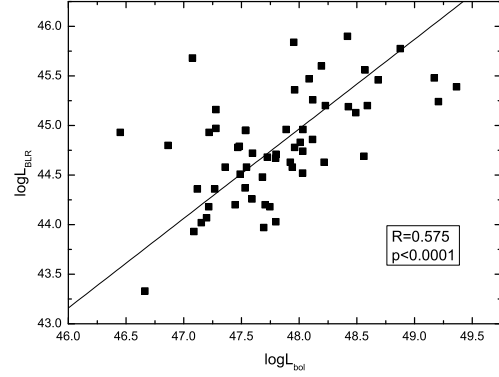


Figure 7. The correlation between $\log L_{BLR}$ and $\log L_{bol}$ for FSRQs. The solid line is the best linear fitting ($p < 0.0001$).

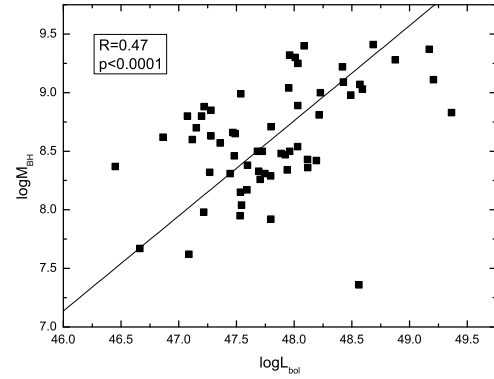


Figure 8. The correlation between $\log M_{BH}$ and $\log L_{bol}$ for FSRQs. The solid line is the best linear fitting ($p < 0.0001$).

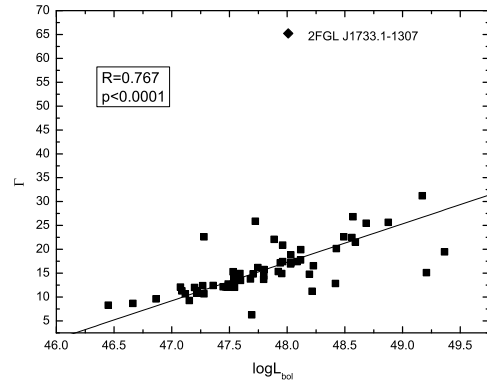


Figure 9. The correlation between Γ and $\log L_{bol}$ for FSRQs. The solid line is the best linear fitting ($p < 0.0001$).

5 DISCUSSIONS AND CONCLUSION

5.1 The effect of the inaccurate redshift of BL Lacs in related linear correlation analysis

Redshifts are normally obtained by spectroscopic and photometric measurement. However, BL Lacs typically lack emission lines. Clear spectroscopic measurements can be obtained for only a small proportion of BL Lacs. Most redshifts of BL Lacs are obtained by photometric measurement or are based on dubious private communications. In Plotkin et al. (2008), photometric redshifts were estimated to be accurate to $\Delta z \approx 0.01$ from comparison with spectroscopic redshifts. However, the two types of redshift measured for a few BL Lacs have a huge difference, $\Delta z \approx 0.5$. The use of inaccurate redshifts may have a significant effect on the calculation of the luminosity and peak frequency in rest-frame.

In this paper, the inaccurate redshifts may affect the correlation between $\log \nu_{peak}^{syn}$ and $-1/c_{syn}$ and between $\log L_{IC}$ and $\log L_{syn}$, discussed in Sect. 4.1 and Sect. 4.2, respectively. In subsamples A and B, there are 17 BL Lacs without measured redshifts. Therefore, we discuss the effect of the inaccurate redshift for two scenarios: (i) all BL Lacs in subsamples A and B. (ii) BL Lacs with measured redshifts in subsamples A and B. On the basis of the redshifts in our sample, we add a normally distributed disturbance. The mean value of this normally distributed disturbance ($\mu_{disturbance}$) are 10% z , 20% z , **30% z** , **40% z** and **50% z** , respectively. The standard deviation (σ) are 10% $\times 0.3144$, 20% $\times 0.3144$, 30% $\times 0.3144$, 40% $\times 0.3144$ and 50% $\times 0.3144$ (0.3144 is the standard deviation of the redshift distribution of BL Lacs in 2LAC). We can then obtain random redshifts and calculate $\log L_{syn}$, $\log L_{IC}$ and $\log \nu_{peak}^{syn}$ in rest-frame. Finally, we repeated the linear correlations 5000 times and analysed the distributions of the coefficient of correlation R , the significance level p and slope K . The results are given in Table 1 to 4.

Table 1 and 2 show the distributions of R , p and K for the correlation between $\log \nu_{peak}^{syn}$ and $-1/c_{syn}$ for all BL Lacs and for BL Lacs with a measured redshift in subsample A. From Tables 1 and 2, it can be seen that all p -values are less than 0.0001 and that all the distributions of R are normally distributed. The mean values of R (μ_R) in Table 1 are almost 0.701 and those of μ_R in Table 2 are almost 0.66. Furthermore, all the standard deviation of R (σ_R) are small, $\sigma_R \leq 0.02$. It can also be seen that all the distributions of K are normal. Their mean values (μ_K) are 1.87 and 1.89, respectively. Their standard deviations are all small, $\sigma_K \leq 0.01$. Table 3 and 4 show the distributions of R , p and K for the correlation between $\log L_{IC}$ and $\log L_{syn}$ for all BL Lacs and for BL Lacs with measured redshift in subsample B. From these two table, it can be seen that almost all the p -values are less than 0.0001, but the distributions of R are not normal any more. In the correlation between $\log L_{IC}$ and $\log L_{syn}$, the coefficient of R is 0.901. Therefore, we want to know how many R -values range between 0.85 and 0.95 after repeating the same linear correlation analysis 5000 times. In these two tables it can be seen that fewer and fewer R -values are in the range between 0.85 and 0.95 with increasing disturbance. The smallest percentage is 61.0%. If we expand the range to 0.8~0.95, the percentage of R for the case of the largest disturbance will rise to 83.1%. All the distributions of slope K are normal, and their mean values (μ_K) are in the

range between 1.05 and 1.16. Their standard deviation (σ_K) are less than 0.08.

In light of the above analysis, we suggest that the effect of the inaccurate redshift is small for the results obtained in Sect. 4.1 and Sect. 4.2. Even if a sample contains a small amount of BL Lacs without measured redshift, our main results will not change. The correlation between $\log \nu_{peak}^{syn}$ and $-1/c_{syn}$ for BL Lacs can still be explained by stochastic particle acceleration mechanisms. In addition, the IC component of BL Lacs can also be considered as an SSC process. However, this conclusion only applies to our sub-sample. It is possible that, if the sample size or the disturbance of redshift increase, our results will be completely different.

5.2 Particle acceleration mechanisms for FSRQ and BL Lac

The correlation between $\log \nu_{peak}^{syn}$ and $-1/c_{syn}$ can be explained in two different scenarios, namely the statistical (energy-dependent acceleration probability and fluctuation of fractional acceleration gain) and the stochastic acceleration mechanisms.

FSRQ and BL Lac, the two different blazar subclasses have many differences. These include (Giommi et al. 2012b): (i) different optical spectral; (ii) different extended radio powers; (iii) very different redshift distributions; (iv) different cosmological evolutions; (v) widely different mix of FSRQs and BL Lac objects in radio and X-ray selected samples; (vi) widely different distributions of the synchrotron peak energy ν_{peak}^S . Therefore, in this paper, we collect a large sample and separate them into FSRQs ($N=200$) and BL Lacs ($N=79$) in order to study the linear correlations between $\log \nu_{peak}^{syn}$ and $-1/c_{syn}$, respectively. For BL Lacs, the slope of the correlation ($k_{BL Lac} = 1.87 \pm 0.19$) is consistent with the stochastic acceleration mechanisms. However, for FSRQs, the slope of the correlation ($k_{FSRQ} = 3.69 \pm 0.24$) has a big difference. It is not consistent with any theoretical values ($k=5/2$, $10/3$ and 2) and cannot be explained by the two particle acceleration mechanisms (Chen 2014).

Chen (2014) used a sample of 43 blazars in order to study the linear correlation between $\log \nu_{peak}^{syn}$ and $-1/c_{syn}$. The slope of the correlation was 2.04 ± 0.03 , which is consistent with the stochastic acceleration mechanisms. The number of objects in the sample was too small to separate them into FSRQs and BL Lacs. Moreover, the correlation was based on only eight HSP blazars. Perhaps this is why he did not find different slopes between FSRQs and BL Lacs.

As noted above, the slope of BL Lacs is consistent with the results of Chen (2014) and can be explained by stochastic particle accelerations. For FSRQs, the slope of the correlation $k_{FSRQ} = 3.69 \pm 0.24$ is close to $10/3$, which can be explained by statistical particle acceleration for the case of fluctuation of fractional acceleration gain. Tramacere et al. (2011) pointed out that the statistic method does not give a complete physical description of the processes responsible for the systematic and stochastic energy gain, as it ignores various physical processes. Thus the slope of the correlation that we found for FSRQs implies that some physical processes may cause error in statistic method. Even so, from the perspective of particle acceleration mechanisms, FSRQs are different from BL Lacs. As far as we know, in terms of the particle acceleration mechanisms, this is the first time that

Table 1. The distribution of R, p and K in the correlation between $\log\nu_{peak}^{syn}$ and $-1/c_{syn}$ for all BL Lacs in sub-sample A.

$\mu_{disturbance}$	μ_R σ_R	The percentage of $p < 0.0001$	μ_K σ_K
50%z	0.700 0.01	100%	1.87 0.01
40%z	0.700 0.004	100%	1.87 0.01
30%z	0.701 0.003	100%	1.87 0.01
20%z	0.702 0.002	100%	1.87 0.005
10%z	0.702 0.001	100%	1.87 0.002

Table 2. The distribution of R, p and K in the correlation between $\log\nu_{peak}^{syn}$ and $-1/c_{syn}$ for BL Lacs with measured redshift in sub-sample A.

$\mu_{disturbance}$	μ_R σ_R	The percentage of $p < 0.0001$	μ_K σ_K
50%z	0.65 0.02	100%	1.89 0.04
40%z	0.66 0.01	100%	1.89 0.03
30%z	0.67 0.01	100%	1.89 0.02
20%z	0.67 0.01	100%	1.89 0.01
10%z	0.66 0.003	100%	1.89 0.01

a difference between FSRQs and BL Lacs has been found by using a large sample. Our results can provide an observational information that is relevant to particle acceleration models.

5.3 EC vs SSC and Curvature of FSRQ

A typical SED of blazars displays two peaks. The high-energy component is usually explained as arising from IC scattering of the same electrons as produce the synchrotron emission. Depending on the origin of the soft photons, the IC scattering can be divided into EC and SSC components. According to Ghisellini et al. (1996), there are two relations that can determine whether the high-energy component is dominated by EC or SSC ($L_{EC} \sim L_{syn}^{1.5}$, $L_{SSC} \sim L_{syn}^{1.0}$). Here we study the correlation between $\log L_{IC}$ and $\log L_{syn}$ for FSRQs and BL Lacs in our subsamples. For FSRQs, the slope of the best linear regression is 1.45 ± 0.11 ; this suggests that the high-energy component of FSRQs is dominated by the EC process (Ghisellini et al. 2002; Celotti & Ghisellini 2008; Ghisellini et al. 2010; Finke 2013). The result of BL Lacs ($k_{BL Lac} = 1.12 \pm 0.10$) suggest that the high-energy component is dominated by the SSC process (Zhang et al. 2013; Lister et al. 2011; Celotti & Ghisellini 2008; Ghisellini et al. 2002; Ghisellini et al. 2010; Ackermann et al. 2012).

When characterizing the two components of the SEDs of blazars, the curvature is another important parameter. It can represent the value of bolometric flux/luminosity if

the peak frequency and peak flux/luminosity are known. By studying the correlation between $\log L_{BLR}$ and $-1/c$, we found that there is no correlation for synchrotron component but that the IC component shows a significant correlation. The synchrotron component is generally explained by synchrotron emission from relativistic electrons in a jet (Maraschi, Ghisellini & Celotti 1992; Massaro et al. 2006; Hovatta et al. 2009), which means that there is no correlation between $\log L_{BLR}$ and $-1/c_{syn}$. The origin of soft photons in IC scattering is complex. In one of the EC models, the soft photons could come from the BLR (Sikora et al. 1994; Dermer et al. 1997). The significant correlation between $\log L_{BLR}$ and $-1/c_{IC}$ that we found might suggest that the soft photons of IC scattering are indeed mainly from the BLR.

In addition, we studied the correlation between $-1/c$ and the $\log L_{bol}$, $\log M_{BH}$ and Γ . Coincidentally, all these parameters have a significant correlation with $-1/c_{IC}$ and no correlation with $-1/c_{syn}$. Perhaps there is a deep-seated physical signification, or maybe it is just a statistical coincidence.

5.4 Jet of FSRQ

In current theoretical models of the formation of jet, power is generated through accretion and the extraction of rotational energy of disc/black hole (Blandford & Znajek 1977; Blandford & Payne 1982) and is then converted into the kinetic power of jet.

Table 3. The distribution of R, p and K in the correlation between $\log L_{IC}$ and $\log L_{syn}$ for all BL Lacs in sub-sample B.

$\mu_{disturbance}$	the percentage of $R \in (0.85, 0.95)$	the percentage of $p < 0.0001$	μ_K σ_K
50%z	70.0%	99.7%	1.05 0.07
40%z	74.9%	99.9%	1.06 0.06
30%z	82.2%	100%	1.07 0.05
20%z	92.9%	100%	1.09 0.04
10%z	98.5%	100%	1.12 0.03

Table 4. The distribution of R, p and K in the correlation between $\log L_{IC}$ and $\log L_{syn}$ for BL Lacs with measured redshift in sub-sample B.

$\mu_{disturbance}$	the percentage of $R \in (0.85, 0.95)$	the percentage of $p < 0.0001$	μ_K σ_K
50%z	61.0%	95.1%	1.09 0.08
40%z	66.0%	97.3%	1.10 0.08
30%z	77.7%	99.3%	1.11 0.07
20%z	90.9%	100%	1.13 0.06
10%z	99.5%	100%	1.16 0.04

Bolometric luminosity is one of the most important parameters of blazars and can function as an index of the jet power (Du et al. 2016). The broad-line luminosity can be taken as an indicator of accretion power (Celotti, Padovani & Ghisellini 1997). Black holes will be spun up through accretion, as these objects acquire mass and angular momentum simultaneously through accretion (Chai, Cao & Gu 2012). The presence of the jet implies that the gravitational potential energy of the falling matter not only can be transformed into heat and radiation, but can also amplify the magnetic field, allowing the field to access the large store of black hole rotational energy and transform part of it into the mechanical power of the jet, as discussed by Ghisellini et al. (2014). These authors predicted that jet power is depended on $(aMB)^2$, where a and M are respectively the spin and mass of the black hole and B is the magnetic field at its horizon.

In our work, the correlations between $\log L_{bol}$ and M_{BH} , L_{BLR} are significant. Our results show that the jet is correlated both with black hole and the accretion disc, which suggest that the origin of jet is a mixture of the mechanisms proposed by Blandford & Znajek and by Blandford & Payne (Punsly & Coroniti 1990; Meier et al. 1999, 2001). Furthermore, the coefficient of the $L_{BLR} \sim L_{bol}$ correlation is 0.9032, very close to 1. This result is consistent with Xie et al. (2007) ($(\log L_{BLR} = \log L_{jet} + \log \eta + \text{const})$). The correlation between $\log L_{bol}$ and Γ can reflect the $P_{power}^{jet} \sim \Gamma$ relationship. Our result shows that the correlation between

$\log L_{bol}$ and Γ is significant, and thus the correlation between P_{power}^{jet} and Γ is significant, too. From the results concerning $L_{bol} \sim \Gamma$ and $L_{bol} \sim M_{BH}$, we found that more powerful jets, the plasma blob in jets will move faster (Kharb et al. 2010; Wu et al. 2011; Lü et al. 2012) and have larger black hole masses (Xiong et al. 2014a). In other words, FSRQs with a larger black hole mass have faster jets ($M_{BH} \sim \Gamma$). According to Maraschi & Tavecchio 2003 ($\delta \sim \Gamma$), the Doppler factor (δ) is also the indicator of the jet speed, so $M_{BH} \sim \delta$ can be used to represent $M_{BH} \sim \Gamma$. In Arshakian et al. (2005), the significant correlation between M_{BH} and δ was found using a sample of 12 objects. Torrealba et al. (2008) obtained the same result using the 15 objects.

ACKNOWLEDGMENTS

We thank the anonymous referee for insightful comments and constructive suggestions. Part of this work is based on archival data, software or online services provided by the ASI SCIENCE DATA CENTER (ASDC). We are very grateful to professor Giommi and supporting team in ASDC for their help. This work is supported by the Joint Research Fund in Astronomy (Grant Nos U1431123, 11263006, 11463001) under cooperative agreement between the National Natural Science Foundation of China (NSFC) and Chinese Academy of Sciences (CAS), the Provincial Natural Science Foundation of Yunnan (Grant No.: 2013FZ042) and

the Yunnan province education department project (Grant No. 2014Y138).

REFERENCES

- Abdo A.A., Ackermann M., Ajello M., et al., 2009, *ApJ*, 700, 597
- Abdo A.A., Ackermann M., Agudo I., et al., 2010a, *ApJ*, 716, 30
- Abdo A.A., Ackermann m., Ajello M., et al., 2010b, *ApJ*, 710, 1271
- Abdo A.A., Ackermann m., Ajello M., et al., 2010c, *ApJ*, 715, 429
- Acciari, V. A., Arlen, T., Aune, T., et al., 2011, *ApJ*, 729, 2
- Ackermann M., Ajello M., Allafort A., et al., 2011, *ApJ*, 743, 171
- Ackermann M., Ajello M., Ballet J., et al., 2012, *ApJ*, 751, 159
- Ackermann M., Ajello M., Atwood W. B., et al., 2015, *ApJ*, 810, 14
- Ackermann M., Ajello M., Allafort A., et al., 2015, Erratum of 2LAC, to be submitted.
- Arbeiter C., Pohl M., et al., 2002, *AAP*, 386, 415
- Arshakian T. G., Chavushyan V. H., Ros E., et al., 2005, *MmSAI*, 76, 35
- Blandford R. D., & Payne D. G., 1982, *MNRAS*, 199, 883
- Blandford R. D., & Znajek R. L., 1977, *MNRAS*, 179, 433
- Blazejowski M., Sikora M., et al., 2000, *ApJ*, 545, 107
- Bloom S. D. & Marscher A. P., 1996, *ApJ*, 461, 657
- Cao X., & Jiang D.R., 1999, *MNRAS*, 307, 802
- Celotti A., Padovani P., & Ghisellini G., 1997, *MNRAS*, 286, 415
- Celotti A., & Ghisellini G., 2008, *MNRAS*, 385, 283
- Chai B., Cao X., & Gu M., 2012, *ApJ*, 759, 114
- Chen L., 2014, *ApJ*, 788, 179
- Chen Y. Y., Zhang X., Zhang H. J., & Yu X. L., 2015, *MNRAS*, 451, 4193
- Dermer C. D., Schlickeiser R. et al., 1992, *A&A*, 256, 27
- Dermer C. D. & Schlickeiser R., 1993, *ApJ*, 416, 458
- Dermer C. D., Sturmer S. J. et al., 1997, *ApJS*, 109, 103
- Donato D., Ghisellini G., Tagliaferri G., Fossati G., 2001, *A&A*, 375, 739
- Du L. M., Xie Z. H., Yi T. F. et al., 2016, *NewA*, 46, 9
- Falcke H., & Biermann P.L., 1995, *A&A*, 293, 665
- Fan J. H., Xie G. Z., & Bacon R., 1999, *A&AS*, 136, 13
- Finke J. D., 2013, *ApJ*, 763, 134
- Fossati G., Celotti A., Ghisellini G., & Maraschi L., 1997, *MNRAS*, 289, 136
- Ghisellini G., 1996, *IAUS*, 175, 413
- Ghisellini G. et al., 1997, *A&A*, 327, 61
- Ghisellini G. et al., 2002, *A&A*, 386, 833
- Ghisellini G., Tavecchio F., & Ghirlanda G., 2009a, *MNRAS*, 399, 2041
- Ghisellini G., Tavecchio F., Foschini L., Ghirlanda G., Maraschi L., & Celotti A., 2009b, *MNRAS*, 402, 497
- Ghisellini G., Tavecchio F., Foschini L., Ghirlanda G., Maraschi L., & Celotti A. 2010, *MNRAS*, 402, 497
- Ghisellini G., Tavecchio F., Foschini L., & Ghirlanda G., 2011, *MNRAS*, 414, 2674
- Ghisellini G., Tavecchio F., Maraschi L., & Sbarrato T., 2014, *Nature*, 515, 376
- Giommi P., Polenta G. et al., 2012, *A&A*, 541, A160
- Giommi P., Padovani P., Polenta G. et al., 2012, *MNRAS*, 420, 2899
- Gu M., Cao X., & Jiang D.R., 2009, *MNRAS*, 396, 984
- Harvey P. M., Wilking B. A., and Joy M., 1982, *ApJ(Letters)*, 254, L29
- Hovatta T., Valtaoja E. et al., 2009, *AAP*, 494, 527
- Jones T. W. et al., 1974, *ApJ*, 188, 353
- Kharb, P., Lister, M. L., & Cooper, N. J., 2010, *ApJ*, 710, 764
- Landau R., 1983, *ApJ*, 268, 68
- Landau R., Golisch, Bill. et al., 1986, *ApJ*, 308, 78
- Liang E. W. & Liu H. T., 2003, *MNRAS*, 340, 632
- Lister M. L., et al. 2011, *ApJ*, 742, 27
- Liu Y., Jiang D.R., & Gu M.F., 2006, *ApJ*, 637, 669
- Lü J., Zou Y. Ch. et al., 2012, *ApJ*, 751, 49
- Maraschi L., Ghisellini G., & Celotti A., 1992, *ApJL*, 397, L5
- Maraschi L. & Tavecchio F., 2003, *ApJ*, 593, 667
- Marscher, A. P. 2009, [arXiv0909.2576M]
- Marscher A. P., & Gear, W. K., 1985, *ApJ*, 298, 114
- Massaro E., Perri M., Giommi P. et al., 2004a, *A&A*, 413, 489
- Massaro E., Perri M., Giommi P. et al., 2004b, *A&A*, 422, 103
- Massaro E., Tramacere A., Perri M. et al., 2006, *A&A*, 448, 861
- Massaro F., Tramacere A., Cavaliere A. et al., 2008, *A&A*, 478, 395
- Meier D. L., 1999, *ApJ*, 522, 753
- Meier D. L., 2001, *ApJL*, 548, L9
- Meyer E. T., Fossati G. et al., 2012, *ApJ*, 752, L4
- Nemmen R. S., Georganopoulou M., Guiriec S. et al., 2012, *Science*, 338, 1445
- Netzer H., 1990, *Active Galactic Nuclei*, 57
- Paggi A., Cavaliere A. et al., 2009a, *A&A*, 508, L31
- Paggi A., Massaro F. et al., 2009b, *A&A*, 504, 821
- Plotkin R. M., Anderson, S. F., Hall P. B. et al. 2008, *AJ*, 135, 2453
- Punsly B., & Coroniti F. V., 1990, *ApJ*, 354, 583
- Rani B., Gupta A. C. et al., 2011, *MNRAS*, 417, 1881
- Rawlings S., & Saunders R., 1991, *Nature*, 349, 138
- Rees M. J., 1967, *MNRAS*, 137, 429
- Sbarrato T., Ghisellini G., Maraschi L., & Colpi M., 2012, *MNRAS*, 421, 1764
- Schneider P., 1993, *A&A*, 269, L13
- Serjeant S., Rawlings S., & Maddow S. J., 1998, *MNRAS*, 294, 494
- Shaw M. S., Romani R. W., Cotter G. et al., 2012, *ApJ*, 748, 49
- Sikora M., Begelman M. C., 1994, *ApJ*, 421, 153
- Stein W. A., Odell S. L., & Strittmatter P. A., 1976, *ARA&A*, 14, 173
- Stickel, M., Padovani, P., Urry, C. M., Fried, J. W., & Kuehr, H. 1991, *ApJ*, 374, 431
- Stratta, G., Capalbi, M., Giommi, P. et al., 2011 [arXiv:1103.0749]
- Torrealba J., Chavushyan V. H., Arshakian T. G., et al. 2008, *RMxAC*, 32, 48
- Tramacere A., Giommi P. et al., 2007, *A&A*, 467, 501

- Tramacere A., Massaro F. et al., 2007, A&A, 466, 521
Tramacere A., Giommi P. et al., 2009, A&A, 501, 879
Tramacere A., Massaro E. et al., 2011, ApJ, 739, 66
Urry C.M & Padovani P., 1995, PASP, 107, 803
Wang J.M., Luo B., & Ho L.C., 2004, ApJ, 615, L9
Woo J.H., & Urry C.M., 2002, ApJ, 579, 530
Wu Q.W., Zou Y.C., Cao X.W. et al., 2011, ApJ, 740, L21
Xie G.Z., Zhou S.B., & Liang E.W., 2004, AJ, 127, 53
Xie G.Z., Dai H., & Zhou S.B., 2007, AJ, 134, 1464
Xiong D. R., Zhang X. et al., 2014, MNRAS, 441, 3375
Xiong D. R., Zhang X. et al., 2014, Ap&SS, 352, 809
Yu X. L., Zhang X. et al., 2015, Ap&SS, 357, 14
Zhang J., Liang E.W., Zhang S.N., & Bai J.M., 2012, ApJ, 752, 157
Zhang J. et al., 2013, ApJ, 767, 8

Table 5. The sample.

Fermi name	Z	time	$Log\nu_{syn}^{peak}$	c_{syn}	$logM_{BH}$	$logL_{BLR}$	Γ	$LogL_{syn}$	$logL_{bol}$	Blazar type.
(1)	(2)	(3)	(4)	(5)	Ref. (6)	Ref. (7)	Ref. (8)	$LogL_{IC}$ (9)	(10)	(11)
2FGL J0004.7-4736	0.88	2010/5/27-2010/6/4	13.22	-0.17	7.85	-	11.77	46.78	-	FSRQ-LSP
2FGL J0006.1+3821	0.229	2010/5/27-2010/6/4	13.05	-0.26	-	-	-	45.76	-	FSRQ-LSP
2FGL J0011.3+0054	1.4934	2010/6/23	13.25	-0.20	7.8, 7.09	-	13	47.02	-	FSRQ-LSP
2FGL J0017.4-0018	1.574	2010/6/24	12.95	-0.12	8.55, 9.04	-	14.53	46.57	47.90	FSRQ-LSP
2FGL J0017.6-0510	0.226	2010/6/22	13.29	-0.19	7.55	-	6.53	45.27	-	FSRQ-LSP
2FGL J0023.2+4454	1.062	2010/1/12	13.49	-0.14	7.78	-	11.98	46.38	-	FSRQ-LSP
2FGL J0030.2-4223	0.495	2010/6/7-2010/6/8	13.55	-0.13	-	-	-	46.01	-	FSRQ-LSP
2FGL J0038.3-2457	1.196	2010/6/19	12.77	-0.25	-	-	-	46.98	-	FSRQ-LSP
2FGL J0043.7+3426	0.966	2010/1/12	-	-	8.01	44.02	13	-	-	FSRQ
2FGL J0046.7-8416	1.032	2010/4/2-2010/4/6	13.15	-0.17	8.68	-	12.52	46.61	-	FSRQ-LSP
2FGL J0047.9+2232	1.161	2010/1/8	13.96	-0.12	8.43, 8.25	-	14.67	46.16	-	FSRQ-LSP
2FGL J0049.7-5738	1.797	2010/5/26-2010/6/10	12.95	-0.15	-	-	-	47.38	47.85	FSRQ-LSP
2FGL J0050.1-0452	0.922	2010/6/30	13.22	-0.16	8.2	-	10.61	46.24	-	FSRQ-LSP
2FGL J0051.0-0648	1.975	2009/5/17	12.62	-0.21	-	-	-	47.33	48.25	FSRQ-LSP
2FGL J0057.9+3311	1.369	2010/1/13-2010/1/14	13.10	-0.20	8.01, 7.97	44.21	13.42	46.53	-	FSRQ-LSP
2FGL J0102.3+4216	0.874	2010/1/17-2010/1/19	13.05	-0.25	7.92, 7.49	-	12	46.40	-	FSRQ-LSP
2FGL J0102.7+5827	0.644	2010/1/23	12.93	-0.20	7.57	-	11	46.83	-	FSRQ-LSP
2FGL J0105.0-2411	1.747	2010/6/25-2010/7/4	12.77	-0.29	8.85, 8.97	-	15.98	47.24	-	FSRQ-LSP
2FGL J0108.6+0135	2.107	2010/7/10	13.02	-0.17	8.83	46.13	28.47	47.89	-	FSRQ-LSP
2FGL J0109.9+6132	0.785	2010/1/31-2010/2/3	12.73	-0.28	-	-	-	46.97	48.15	FSRQ-LSP
2FGL J0112.8+3208	0.603	2009/8/31	0.00	-0.14	-	-	-	48.12	-	FSRQ
2FGL J0113.7+4948	0.395	2010/8/27	13.39	-0.15	8.34	-	7.34	46.08	46.44	FSRQ-LSP
2FGL J0116.0-1134	0.671	2010/6/7	13.49	-0.12	8.57, 8.92	-	2	46.18	-	FSRQ-LSP
2FGL J0118.8-2142	1.165	2010/6/29-2010/7/4	13.17	-0.19	10	-	-	46.65	-	FSRQ-LSP
2FGL J0132.8-1654	1.02	2010/7/7-2010/8/4	13.64	-0.14	-	-	-	47.10	-	FSRQ-LSP
2FGLJ0136.9+4751	0.859	2010/2/5	12.84	-0.18	8.73, 8.3	-	-	47.24	-	FSRQ-LSP
2FGL J0137.6-2430	0.835	2010/7/2-2010/7/6	13.25	-0.15	9.11, 9.13	-	11.87	47.30	47.99	FSRQ-LSP
2FGL J0145.1-2732	1.148	2010/7/2-2010/7/6	13.09	-0.16	-	-	2	47.90	-	FSRQ-LSP
2FGL J0158.0-4609	2.287	2010/5/2	12.92	-0.18	7.98, 8.52	-	16.85	46.89	-	FSRQ-LSP
2FGL J0205.3-1657	1.466	2010/1/8	12.85	-0.09	1	-	2	46.96	-	FSRQ-LSP
2FGL J0206.5-1149	1.663	2010/1/12-2010/1/13	13.74	-0.16	-	-	-	47.84	-	FSRQ-LSP
2FGL J0217.7+7353	2.367	2010/9/10-2010/9/11	12.74	-0.17	-	-	-	47.05	47.98	FSRQ-LSP
2FGL J0217.5-0813	0.607	2010/3/5	12.84	-0.09	-	-	-	47.93	-	FSRQ-LSP
2FGLJ0217.9+0143	1.715	2010/1/29-2010/2/2	13.22	-0.16	-	-	-	47.23	-	FSRQ-LSP
2FGL J0221.0+3555	0.944	2010/8/4-2010/8/20	13.00	-0.21	-	-	-	47.81	50.07	FSRQ-LSP
2FGL J0222.0-1615	0.7	2010/5/30	13.32	-0.11	-	-	-	50.07	-	FSRQ-LSP
2FGL J0229.3-3644	2.115	2010/6/7	12.98	-0.22	6.53	-	7.8	46.14	-	FSRQ-LSP
2FGL J0230.8+4031	1.019	2010/6/3	13.07	-0.18	1	-	2	46.14	-	FSRQ-LSP
2FGL J0237.1-6136	0.467	2010/6/12-2010/6/16	13.56	-0.17	-	-	-	47.89	48.26	FSRQ-LSP
2FGLJ0237.8+2846	1.213	2010/2/5	13.29	-0.17	9.22	45.9	12.86	48.01	-	FSRQ-LSP
2FGL J0245.1+2406	2.247	2010/02/01-2010/3/11	13.66	-0.10	9.12, 9.18	-	20.88	47.62	48.42	FSRQ-LSP
2FGL J0245.9-4652	1.385	2010/7/3-2010/7/8	13.68	-0.10	1	-	2	48.34	-	FSRQ-LSP
2FGL J0250.6+1713	1.1	2010/1/30	13.82	-0.13	8.48, 8.32	-	20.21	46.87	48.94	FSRQ-LSP
2FGL J0252.7-2218	1.419	2010/6/7	13.08	-0.15	1	-	2	48.93	-	FSRQ-LSP
2FGL J0253.5+5107	1.732	2010/2/10	12.77	-0.17	9.4	-	19.47	47.32	-	FSRQ-LSP
2FGL J0257.7-1213	1.391	2010/1/22	13.52	-0.18	1	-	2	46.06	-	FSRQ-LSP
2FGL J0259.5+0740	0.893	2010/1/29	13.07	-0.19	9.11, 7.37	-	14	46.92	-	FSRQ-LSP
2FGL J0302.7-7919	1.053	2010/4/15	13.10	-0.20	3	-	3	46.64	-	FSRQ-LSP
2FGL J0303.5-6209	1.348	2010/6/12	12.92	-0.14	9.22	45.14	13.2	46.64	-	FSRQ-LSP
2FGL J0310.0-6058	1.479	2010/6/19	13.11	-0.15	2	-	2	46.46	-	FSRQ-LSP
2FGL J0310.7+3813	0.816	2010/2/9	12.74	-0.20	-	-	-	46.52	-	FSRQ-LSP
				-0.18	9.76	-	15.43	47.23	-	FSRQ-LSP
				-	1	-	2	47.25	-	FSRQ-LSP
				-0.17	8.87	44.88	16.68	47.25	-	FSRQ-LSP
				-0.22	2	2	2	46.34	-	FSRQ-LSP
				-	8.23	43.82	9.76	46.34	-	FSRQ-LSP
				-	2	2	2	-	-	

Table 5. Continued.

Fermi name	Z	time	$Log\nu_{syn}^{peak}$	c_{syn}	$log M_{BH}$	$log L_{BLR}$	Γ	$Log L_{syn}$	$log L_{bol}$	Blazar type.
(1)	(2)	(3)	(4)	(5)	Ref. (6)	Ref. (7)	Ref. (8)	$Log L_{IC}$ (9)	(10)	(11)
2FGL J0315.8-1024	1.565	2010/1/28	13.05	-0.17	7.17, 8.33	44.67	7.23	46.38	-	FSRQ-LSP
2FGL J0326.1+2226	2.066	2010/2/8	13.43	-0.16	9.5, 9.16	45.81	20.67	47.77	-	FSRQ-LSP
2FGLJ0337.0+3200	1.259	2010/1/17	-	-	9.25	45.93	27.48	-	-	FSRQ
2FGL J0342.4+3859	0.945	2010/2/15-2010/2/16	13.65	-0.17	7.42	43.87	12.11	46.28	-	FSRQ-LSP
2FGLJ0350.0-2104	2.944	2008/10/15	-	-	9.08, 9.07	45.25	8.59	46.49	-	FSRQ-LSP
2FGL J0405.8-1309	0.571	2010/2/9-2010/2/10	13.47	-0.11	8.65	44.51	12.73	46.78	47.49	FSRQ-LSP
2FGL J0407.7+0740	1.133	2010/2/14-2010/2/15	12.99	-0.22	7.83	44.14	13.08	-	-	FSRQ
2FGL J0413.5-5332	1.024	2009/10/17	-	-	7.47	43.42	5.79	45.52	-	FSRQ-LSP
2FGL J0422.1-0645	0.242	2010/2/14	14.12	-0.13	9.03, 9, 8.41	44.63	11.2	47.84	48.22	FSRQ-LSP
2FGL J0423.2-0120	0.916	2009/8/27	13.41	-0.14	8.66	44.78	12.11	46.75	47.47	FSRQ-LSP
2FGL J0439.0-1252	1.285	2010/7/1	13.07	-0.08	8.8	-	-	47.18	47.90	FSRQ-LSP
2FGLJ0457.0-2325	1.003	2010/2/25	13.20	-0.16	9.27, 8.66	45.3	16.57	47.79	-	FSRQ-LSP
2FGL J0501.2-0155	2.291	2010/2/27	13.53	-0.12	8.74	44.86	13.62	46.58	-	FSRQ-LSP
2FGL J0507.5-6102	1.089	2010/1/20	13.54	-0.12	8.02	-	4.86	45.26	-	FSRQ-LSP
2FGL J0516.5-4601	0.194	2010/2/20	13.23	-0.13	10.2, 9.4	-	21.35	-	-	FSRQ
2FGLJ0530.8+1333	2.07	2009/9/24	-	-	8.43	44.86	17.76	47.10	48.12	FSRQ-LSP
2FGL J0532.7+0733	1.254	2010/4/25	12.98	-0.16	8.43	44.86	17.76	47.10	48.12	FSRQ-LSP
2FGLJ0539.3-2841	3.104	2010/3/12	12.87	-0.23	7.36	44.69	22.49	47.71	48.56	FSRQ-LSP
2FGL J0601.1-7037	2.409	2010/3/9	13.58	-0.19	8.43, 8.825	44.97	22.62	46.63	47.28	FSRQ-LSP
2FGL J0608.0-0836	0.872	2010/6/7	12.62	-0.16	8.09	44.51	14.77	46.38	-	FSRQ-LSP
2FGL J0608.0-1521	1.094	2010/3/16-2010/3/23	13.24	-0.18	9.41, 8.81	45.23	12.43	-	-	FSRQ
2FGL J0635.5-7516	0.653	2009/1/13	-	-	8.17	44.26	14.94	46.64	47.59	FSRQ-LSP
2FGL J0654.2+4514	0.928	2010/3/23	13.13	-0.08	7.86, 8.79	43.97	6.3	-	-	FSRQ-LSP
2FGL J0654.5+5043	1.253	2010/1/15	14.01	-0.14	8.82, 8.77	45.68	12.08	46.22	47.07	FSRQ-LSP
2FGL J0656.2-0320	0.634	2010/3/31	12.58	-0.22	7.33, 7.91	43.93	11.3	46.43	47.09	FSRQ-LSP
2FGL J0714.0+1933	0.54	2010/4/2-2010/4/3	13.51	-0.19	8.49, 9.12	45.33	9.41	46.25	-	FSRQ-LSP
2FGL J0721.5+0404	0.665	2010/4/5	12.92	-0.20	8, 8.47, 7.86	44.19	16.57	45.89	-	FSRQ-LSP
2FGL J0739.2+0138	0.189	2010/4/10-2010/4/11	13.76	-0.13	9.59, 9.23	45.46	25.46	47.27	48.68	FSRQ-LSP
2FGL J0746.6+2549	2.979	2010/10/15	12.78	-0.21	8.15	44.95	12.82	47.15	47.53	FSRQ-LSP
2FGL J0750.6+1230	0.889	210/4/1-2010/4/12	12.95	-0.19	9.07	45.56	26.84	47.40	48.57	FSRQ-LSP
2FGL J0805.5+6145	3.033	2010/4/3-2010/4/4	12.79	-0.17	8.55	44.83	12.78	46.86	-	FSRQ-LSP
2FGL J0824.7+3914	1.216	2010/4/13	13.05	-0.13	9.42, 9.1	-	16.34	-	-	FSRQ
2FGLJ0824.9+5552	1.417	2010/3/28	-	-	9.68	43.07	6.52	45.58	-	FSRQ-LSP
2FGL J0834.3+4221	0.249	2010/4/13-2010/4/15	13.67	-0.14	9.36	-	28.15	-	-	FSRQ
2FGL J0841.6+7052	2.218	2010/3/21	-	-	9.25	45.26	12.72	46.93	-	FSRQ-LSP
2FGL J0903.4+4651	1.466	2010/4/18	12.90	-0.12	9.32, 8.55, 9.14	45.2	16.57	47.17	48.23	FSRQ-LSP
2FGL J0909.1+0121	1.024	2010/4/18-2010/5/5	13.44	-0.15	8.7	45.21	20.46	47.14	-	FSRQ-LSP
2FGL J0910.9+2246	2.661	2010/4/28	13.11	-0.22	9.32	45.36	17.42	47.30	47.96	FSRQ-LSP
2FGL J0912.1+4126	2.563	2010/2/25	12.97	-0.31	8.62	44.8	6.52	46.64	-	FSRQ-LSP
2FGL J0917.0+3900	1.267	2010/4/25	12.84	-0.16	9.25, 9.31, 9.29	45.775	25.67	47.83	48.88	FSRQ-LSP
2FGL J0920.9+4441	2.19	2009/10/29	12.97	-0.20	7.68, 8.16	43.75	16.29	46.86	-	FSRQ-LSP
2FGL J0923.2+4125	1.732	2010/4/25-2010/4/26	13.67	-0.13	8.8, 8.825	44.52	10.47	46.32	-	FSRQ-LSP
2FGL J0924.0+2819	0.744	2010/4/29	12.88	-0.19	8.29, 7.5	44.26	5.86	45.60	-	FSRQ-LSP
2FGL J0937.6+5009	0.275	2010/4/21-2010/4/25	12.85	-0.26	8.95	45.5	30.86	46.88	-	FSRQ-LSP
2FGL J0948.8+4040	1.249	2010/4/30	12.68	-0.17	9.34, 9.8.7, 8.465	44.93	11.33	46.60	47.22	FSRQ-LSP
2FGL J0956.9+2516	0.707	2010/5/7-2010/6/15	12.88	-0.19	8.96, 7.87, 8.07, 8.45	44.58	17.16	46.92	47.94	FSRQ-LSP
2FGL J0957.7+5522	0.896	2009/11/1	13.82	-0.10	7.73, 7.86	44.56	19.64	46.42	-	FSRQ-LSP
2FGL J1012.6+2440	1.805	2010/5/11	14.02	-0.10	8.479, 8.54	44.89	9	46.23	-	FSRQ-LSP
2FGL J1014.1+2306	0.566	2010/5/12	13.48	-0.12	9.11, 7.99	44.62	20.18	46.87	-	FSRQ-LSP
2FGL J1016.0+0513	1.713	2010/5/18	12.91	-0.19	9.1	45.34	13.16	46.64	-	FSRQ-LSP
2FGL J1017.0+3531	1.228	2010/5/8	13.04	-0.15	8.65, 8.61	44.48	13.94	47.25	-	FSRQ-LSP
2FGL J1033.2+4117	1.117	2010/5/8-2010/5/9	12.93	-0.20	-	-	-	-	-	-

Table 5. *Continued.*

Fermi name	Z	time	$Log v_{syn}^{peak}$	c_{syn}	$log M_{BH}$	$log L_{BLR}$	Γ	$Log L_{syn}$	$log L_{bol}$	Blazar type.
(1)	(2)	(3)	(4)	(5)	Ref. (6)	Ref. (7)	Ref. (8)	$Log L_{IC}$	(10)	(11)
2FGL J1037.5-2820	1.066	2010/1/22-2010/1/23	13.62	-0.14	8.99	44.95	14.34	46.65	47.54	FSRQ-LSP
				-0.11	2	2	2	47.48		
2FGL J1106.1+2814	0.843	2010/5/24	13.46	-0.18	8.85	45.16	10.7	46.67	47.28	FSRQ-LSP
				-0.10	2	2	2	47.16		
2FGL J1112.4+3450	1.949	2010/5/19-2010/5/25	13.25	-0.21	9.04, 8.78	45.22	19.45	47.34	-	FSRQ-LSP
				-	2	2	2	-		
2FGL J1120.4+0710	1.336	2010/6/5	13.57	-0.14	8.83	44.47	12.85	46.57	-	FSRQ-LSP
				-	2	2	2	-		
2FGL J1124.2+2338	1.549	2010/5/28-2010/5/30	13.01	-0.19	8.79	45.05	14.44	47.00	-	FSRQ-LSP
				-	2	2	2	-		
2FGL J1126.6-1856	1.048	2010/6/10	13.58	-0.13	-	-	-	47.30	47.92	FSRQ-LSP
				-0.09	-	-	-	47.80		
2FGL J1130.3-1448	1.184	2009/12/28	-	-	9.18	-	16.96	-	-	FSRQ
				-0.13	1	-	2	47.99		
2FGL J1146.8-3812	1.048	2010/6/24	12.97	-0.20	8.5	44.48	13.78	47.20	47.68	FSRQ-LSP
				-0.06	2	2	2	47.51		
2FGL J1146.9+4000	1.089	2010/5/25-2010/5/26	13.42	-0.16	8.98, 8.93	45.06	14.94	47.15	-	FSRQ-LSP
				-	2	2	2	-		
2FGL J1152.4-0840	2.367	2010/6/16	13.18	-0.17	9.38	45.25	18.7	47.60	-	FSRQ-LSP
				-	2	2	2	-		
2FGL J1159.5+2914	0.724	2010/5/28-2010/6/11	13.49	-0.13	9.18, 7.9, 8.54, 8.375	44.68	25.9	47.01	47.72	FSRQ-LSP
				-0.08	2	2	2	47.63		
2FGL J1206.0-2638	0.789	2010/6/30-2010/12/10	13.43	-0.12	8.59, 9	44.07	12	46.51	47.20	FSRQ-LSP
				-0.08	2	2	2	47.10		
2FGL J1208.8+5441	1.344	2010/5/16-2010/5/21	13.71	-0.13	8.67, 8.4	44.52	16.95	46.83	48.03	FSRQ-LSP
				-0.12	2	2	2	48.00		
2FGL J1209.7+1807	0.845	2010/6/9-2010/6/11	12.88	-0.25	8.94, 8.515	44.47	9.86	46.18	-	FSRQ-LSP
				-	2	2	2	-		
2FGL J1219.7+0201	0.241	2010/6/24	-	-	8.87	-	6.22	-	-	FSRQ
				-0.08	1	-	2	46.15		
2FGL J1222.4+0413	0.967	2010/6/17-2010/6/29	13.57	-0.13	8.24, 8.37	-	14.94	47.18	48.14	FSRQ-LSP
				-0.15	1	-	2	48.09		
2FGL J1228.6+4857	1.722	2009/2/25-2009/2/26	-	-	9.22, 8.255	44.73	15.71	-	-	FSRQ
				-0.06	2	2	2	47.93		
2FGL J1239.5+0443	1.761	2009/1/2-2009/1/4	-	-	8.67, 8.57	44.9	21.93	-	-	FSRQ
				-0.07	2	2	2	48.33		
2FGL J1246.7-2546	0.635	2010/1/25	12.92	-0.25	9.04	-	14.77	46.77	47.63	FSRQ-LSP
				-0.09	1	-	2	47.57		
2FGL J1256.1-0547	0.536	2010/1/15	12.62	-0.18	8.9, 8.43, 8.4, 8.28	44.78	20.87	47.27	47.96	FSRQ-LSP
				-0.08	1	9	2	47.86		
2FGL J1258.2+3231	0.806	2010/6/13-2010/6/19	13.94	-0.13	8.74, 8.255	44.42	10.09	46.92	-	FSRQ-LSP
				-	2	2	2	-		
2FGL J1303.5-4622	1.664	2010/1/24-2010/1/27	13.70	-0.17	7.95, 8.21	44.21	14.18	47.06	-	FSRQ-LSP
				-	2	2	2	-		
2FGL J1310.6+3222	0.997	2009/12/12-2009/12/21	12.86	-0.14	8.8, 9.24, 7.3, 8.57	44.96	22.1	47.16	47.89	FSRQ-LSP
				-0.08	1	1	2	47.79		
2FGL J1317.9+3426	1.056	2010/6/16-2010/6/20	13.38	-0.16	9.29, 9.14	45.08	10.82	46.74	-	FSRQ-LSP
				-	2	2	2	-		
2FGL J1321.1+2215	0.943	2010/1/7	13.16	-0.19	8.42, 8.315	44.71	12.33	46.68	-	FSRQ-LSP
				-	2	2	2	-		
2FGL J1326.8+2210	1.4	2010/3/30	12.88	-0.19	9.24, 9.25	44.96	17.16	47.10	48.03	FSRQ-LSP
				-0.10	2	2	2	47.98		
2FGL J1332.5-1255	1.492	2010/7/10	12.75	-0.24	8.96, 8.61	45.26	19.63	46.61	-	FSRQ-LSP
				-	2	2	2	-		
2FGL J1332.7+4725	0.668	2010/6/10-2010/6/19	12.83	-0.20	8.56, 7.975	44.32	8.49	45.94	-	FSRQ-LSP
				-	2	2	2	-		
2FGL J1333.5+5058	1.362	2010/3/13	13.79	-0.14	7.95	44.37	15.32	46.33	47.53	FSRQ-LSP
				-0.10	2	2	2	47.50		
2FGL J1337.7-1257	0.539	2010/1/18-2010/1/26	12.94	-0.18	7.98	44.18	10.82	46.80	47.22	FSRQ-LSP
				-0.06	2	2	2	47.00		
2FGL J1344.2-1723	2.506	2010/1/21	13.46	-0.20	9.12	45.02	22.81	47.82	-	FSRQ-LSP
				-	2	2	2	-		
2FGL J1345.4+4453	2.534	2010/6/15-2010/6/19	13.08	-0.16	8.98	45.12	24.47	46.95	-	FSRQ-LSP
				-	2	2	2	-		
2FGL J1345.9+0706	1.093	2010/7/5	13.85	-0.15	8.48	44.61	11.19	46.72	-	FSRQ-LSP
				-	2	2	2	-		
2FGL J1347.7-3752	1.3	2010/9/20	13.77	-0.15	7.95, 8.62	44.67	13.71	46.86	47.80	FSRQ-LSP
				-0.10	2	2	2	47.74		
2FGL J1358.1+7644	1.585	2010/5/24-2010/5/25	12.73	-0.19	8.34, 8.17	44.2	14.87	46.87	47.70	FSRQ-LSP
				-0.08	2	2	2	47.64		
2FGL J1359.4+5541	1.014	2010/6/6-2010/6/8	13.24	-0.22	8	43.99	12.58	46.60	-	FSRQ-LSP
				-	2	2	2	-		
2FGL J1408.8-0751	1.494	2010/5/23	13.29	-0.16	9.4	45.47	17.42	47.33	48.09	FSRQ-LSP
				-0.08	2	2	2	48.00		
2FGL J1419.4+3820	1.831	2010/1/8	12.91	-0.20	8.59, 8.68	45.1	16.38	47.32	-	FSRQ-LSP
				-	2	2	2	-		
2FGL J1436.9+2319	1.548	2010/6/14	13.06	-0.15	8.44, 8.31	44.72	13.48	46.95	47.59	FSRQ-LSP
				-0.07	2	2	2	47.48		
2FGL J1504.3+1029	1.839	2010/7/29	13.33	-0.14	9.64, 8.74, 8.94	45.24	15.11	47.63	49.21	FSRQ-LSP
				-0.11	2	2	2	49.19		
2FGL J1510.9-0545	1.191	2010/2/13-2010/2/19	13.15	-0.15	8.97	-	16.2	47.05	-	FSRQ-LSP
				-	2	2	2	-		
2FGL J1512.8-0906	0.36	2009/1/16	-	-	8.6, 8.65, 8, 8.2	44.65	27.925	-	-	FSRQ
				-0.12	4	4	4	48.00		
2FGL J1514.6+4449	0.57	2010/4/6	13.05	-0.27	7.72, 7.62	43.33	8.66	46.06	46.66	FSRQ-LSP
				-0.09	2	2	2	46.54		
2FGL J1522.0+4348	2.171	2010/1/18	12.79	-0.24	8.59, 8.67	45.49	19.39	47.14	-	FSRQ-LSP
				-	2	2	2	-		
2FGL J1522.1+3144	1.484	2010/1/25-2010/1/28	13.43	-0.11	8.92	44.9	25.82	46.57	-	FSRQ-LSP
				-	2	2	2	-		
2FGL J1539.5+2747	2.191	2010/3/17	13.77	-0.13	8.43, 8.51	44.63	15.33	47.15	47.92	FSRQ-LSP
				-0.04	2	2	2	47.84		
2FGL J1549.5+0237	0.414	2010/2/13-2010/2/20	13.04	-0.18	8.61, 8.72, 8.47, 8.67	44.8	9.64	46.25	46.86	FSRQ-LSP
				-0.09	2	2	2	46.74		
2FGL J1553.5+1255	1.29	2010/2/11	12.93	-0.15	9.1, 8.64	45.19	17.76	46.74	-	FSRQ-LSP
				-	2	2	2	-		
2FGL J1608.5+1029	1.226	2010/2/16-2010/2/17	13.60	-0.12	8.64, 9.5, 8.77	45.04	18.81	47.23	-	FSRQ-LSP
				-	2	2	2	-		
2FGL J1613.4+3409	1.397	2010/6/7	13.89	-0.11	9.12, 9.57, 9.6, 9.08	45.61	8.02	47.64	-	FSRQ-LSP
				-	2	2	2	-		

Table 5. Continued.

Fermi name	Z	time	$Log\nu_{syn}^{peak}$	c_{syn}	$log M_{BH}$	$log L_{BLR}$	Γ	$Log L_{syn}$	$log L_{bol}$	Blazar type.
(1)	(2)	(3)	(4)	c_{IC}^C (5)	Ref. (6)	Ref. (7)	Ref. (8)	$Log L_{IC}$ (9)	(10)	(11)
2FGLJ1625.7-2526	0.786	2010/8/27-2010/9/3	13.05	-0.14	-	-	-	46.92	-	FSRQ-LSP
2FGLJ1635.2+3810	1.814	2010/3/7	12.82	-0.19	9.53, 9.2, 9.67, 9.075	45.48	31.22	47.96	49.17	FSRQ-LSP
2FGL J1637.7+4714	0.735	2010/7/30-2010/7/31	12.85	-0.21	8.61, 8.52	44.58	12.43	46.60	47.36	FSRQ-LSP
2FGLJ1640.7+3945	1.66	2010/8/7	13.18	-0.08	2	2	2	47.27	-	FSRQ-LSP
2FGLJ1642.9+3949	0.593	2010/3/6	-	-0.17	-	-	-	47.38	-	FSRQ-LSP
2FGL J1703.2-6217	1.747	2010/3/12-2010/3/13	13.23	-0.11	7.73, 9.03	45.23	11	-	-	FSRQ
2FGL J1709.7+4319	1.027	2009/12/1	13.39	-0.08	3	8	3	47.42	-	FSRQ-LSP
2FGL J1728.2+0429	0.296	2010/3/12-2010/3/13	13.43	-0.23	8.65, 8.55	45.31	21.47	47.86	-	FSRQ-LSP
2FGL J1733.1-1307	0.902	2010/3/14-2010/4/10	13.45	-0.09	2	2	2	47.76	47.80	FSRQ-LSP
2FGL J1740.2+5212	1.375	2010/3/6-2010/3/11	13.63	-0.14	7.92	44.03	14.44	46.75	-	FSRQ-LSP
2FGL J1818.6+0903	0.354	2010/3/25-2010/3/26	13.71	-0.09	2	2	2	47.88	-	FSRQ-LSP
2FGL J1830.1+0617	0.745	2009/5/20	-	-0.14	9.32	45.16	17.97	47.51	-	FSRQ-LSP
2FGLJ1833.6-2104	2.507	2010/9/23	12.74	-0.17	7.3, 7.5	43.93	8.22	45.67	-	FSRQ-LSP
2FGL J1848.5+3216	0.798	2010/10/6-2010/10/19	13.35	-0.15	2	2	2	47.56	-	FSRQ
2FGL J1849.4+6706	0.657	2010/6/3-2010/7/9	13.58	-0.08	8.69, 8.86	45.45	12.52	48.06	-	FSRQ-LSP
2FGL J1902.5-6746	0.254	2010/3/28-2010/4/6	13.00	-0.07	2	2	2	47.47	-	FSRQ-LSP
2FGLJ1911.1-2005	1.119	2009/10/4	12.88	-0.16	7.87, 8.21	44.58	12.06	46.76	47.54	FSRQ-LSP
2FGLJ1923.5-2105	0.874	2010/9/30	14.04	-0.07	2	2	2	47.47	-	FSRQ-LSP
2FGL J1924.8-2912	0.353	2010/9/30	12.73	-0.19	9.14	44.42	14.27	47.03	-	FSRQ-LSP
2FGL J1954.6-112	0.683	2009/12/3	-	-0.22	2	2	2	47.35	-	FSRQ-LSP
2FGL J1958.2-3848	0.63	2010/4/9-2010/4/14	13.02	-0.11	7.51	43.35	6.13	45.30	-	FSRQ-LSP
2FGL J1959.1-4245	2.178	2010/4/5-2010/4/14	13.41	-0.10	2	2	2	47.46	48.23	FSRQ-LSP
2FGL J2035.4+1058	0.601	2010/5/3-2010/5/7	12.99	-0.08	-	-	-	48.15	-	FSRQ-LSP
2FGLJ2056.2-4715	1.491	2010/10/18	12.91	-0.07	-	-	-	47.57	-	FSRQ-LSP
2FGL J2109.9+0807	1.58	2010/5/13-2010/5/14	13.57	-0.19	9.01, 8.38	44.02	9.3	46.86	47.15	FSRQ-LSP
2FGL J2115.3+2932	1.514	2010/5/25	12.95	-0.17	2	2	2	46.84	-	FSRQ-LSP
2FGL J2121.0+1901	2.18	2009/1/2	-	-0.08	6.73	43.37	12.23	-	-	FSRQ
2FGL J2135.6-4959	2.181	2010/4/22-2010/5/5	13.05	-0.09	2	2	2	47.20	-	FSRQ-LSP
2FGL J2143.5+1743	0.211	2009/1/15	-	-0.17	7.99, 8.63	44.2	12.16	46.75	47.44	FSRQ-LSP
2FGL J2144.8-3356	1.361	2009/9/22-2009/9/24	13.52	-0.11	2	2	2	47.35	-	FSRQ-LSP
2FGLJ2151.5-3021	2.345	2010/5/4-2010/5/13	12.92	-0.20	8.55, 9.41	45.13	22.62	47.45	48.49	FSRQ-LSP
2FGL J2157.4+3129	1.488	2009/7/8-2009/7/12	13.23	-0.07	2	2	2	48.45	-	FSRQ-LSP
2FGL J2157.9-1501	0.672	2010/5/17	13.14	-0.13	7.74, 8.26	44.17	11.46	46.19	-	FSRQ-LSP
2FGL J2201.9-8335	1.865	2010/7/5-2010/7/17	13.31	-0.19	2	2	2	47.62	-	FSRQ-LSP
2FGL J2211.9+2355	1.125	2009/4/15-2009/4/21	12.92	-0.07	9.6	-	-	47.62	-	FSRQ-LSP
2FGL J2219.1+1805	1.071	2010/6/3-2010/6/6	12.41	-0.13	8.74	44.78	16.1	47.09	-	FSRQ-LSP
2FGL J2225.6-0454	1.404	2010/5/22-2010/5/27	12.75	-0.13	2	2	2	48.10	-	FSRQ
2FGLJ2232.4+1143	1.037	2009/11/27-2009/11/29	-	-0.07	7.75	44.26	20.75	-	-	FSRQ
2FGLJ2253.9+1609	0.859	2009/12/4-2009/12/6	12.76	-0.16	2	2	2	48.26	-	FSRQ-LSP
2FGL J2258.0-2759	0.926	2010/5/20-2010/5/26	13.14	-0.13	8.31, 8.4	45.26	19.93	46.68	48.12	FSRQ-LSP
2FGL J2322.2+3206	1.489	2009/5/20	13.05	-0.09	8.6, 8.74, 8.1	44.26	8.8	-	-	FSRQ
2FGL J2327.5+0940	1.841	2010/6/18-2010/6/29	12.64	-0.13	2	2	2	46.60	-	FSRQ-LSP
2FGL J2334.3+0734	0.401	2009/12/20	12.94	-0.17	8.31	44.18	16.18	47.04	47.75	FSRQ-LSP
2FGLJ2345.0-1553	0.621	2009/1/10	13.40	-0.07	2	2	2	47.65	-	FSRQ
2FGL J2347.9-1629	0.576	2009/12/04-2009/12/05	13.07	-0.15	8.87	45.48	7.93	-	-	FSRQ
2FGL J2356.3+0432	1.248	2010/6/22-2010/6/23	12.53	-0.13	1	8	2	47.05	48.86	FSRQ-LSP
				-0.17	-	-	-	47.49	-	FSRQ-LSP
				-0.08	-	-	-	48.84	-	FSRQ-LSP
				-0.15	8.89	44.74	18.82	46.96	48.03	FSRQ-LSP
				-0.08	2	2	2	47.99	-	FSRQ-LSP
				-0.13	7.59	43.68	10.45	46.70	-	FSRQ-LSP
				-	2	2	2	-	-	FSRQ-LSP
				-0.15	9.02, 9.16	45.19	20.18	47.24	48.43	FSRQ-LSP
				-0.12	2	2	2	48.40	-	FSRQ-LSP
				-0.20	8.46	44.79	12.08	46.94	47.48	FSRQ-LSP
				-0.04	2	2	2	47.34	-	FSRQ-LSP
				-0.29	7.65, 7.66	44.07	10.41	46.31	-	FSRQ-LSP
				-	2	2	2	-	-	FSRQ-LSP
				-0.16	8.81, 8.54, 7.9	45.6	14.77	47.68	48.19	FSRQ-LSP
				-0.09	2	2	2	48.03	-	FSRQ
				-	8.7, 8.64, 9	45.58	15.47	-	-	FSRQ
				-0.10	1	8	2	48.00	-	FSRQ
				-0.28	8.7, 9.17, 8.6, 8.83	45.39	19.47	48.30	49.36	FSRQ-LSP
				-0.13	1	8	2	49.32	-	FSRQ-LSP
				-0.17	8.92, 9.16	45.84	14.94	47.33	47.95	FSRQ-LSP
				-0.10	2	2	2	47.83	-	FSRQ-LSP
				-0.16	8.66, 8.75	44.71	15.76	46.69	47.80	FSRQ-LSP
				-0.07	2	2	2	47.76	-	FSRQ-LSP
				-0.24	8.7, 9.35	45.2	21.52	47.22	48.59	FSRQ-LSP
				-0.12	2	2	2	48.57	-	FSRQ-LSP
				-0.17	8.37	44.93	8.3	45.90	46.45	FSRQ-LSP
				-0.06	2	2	2	46.31	-	FSRQ-LSP
				-0.18	8.16, 8.48	44.36	12.4	46.61	47.27	FSRQ-LSP
				-0.08	1	1	2	47.16	-	FSRQ-LSP
				-0.16	8.72, 8.47	44.36	10.7	46.65	47.12	FSRQ-LSP
				-0.06	2	2	2	46.94	-	FSRQ-LSP
				-0.30	8.41, 8.45	45.02	12.64	46.32	-	FSRQ-LSP
				-	2	2	2	-	-	FSRQ-LSP

Table 5. *Continued.*

Fermi name	Z	time	$Log \nu_{syn}^{peak}$	c_{syn}	$log M_{BH}$	$log L_{BLR}$	Γ	$Log L_{syn}$	$log L_{bol}$	Blazar type.
(1)	(2)	(3)	(4)	(5)	Ref. (6)	Ref. (7)	Ref. (8)	$Log L_{IC}$	(10)	(11)
2FGL J0007.8+4713	0.28	2010/1/12	15.23	-0.08	-	-	-	45.31	-	BL Lac-HSP
2FGL J0009.0+0632	0.27	2010/6/25	12.74	-0.14	-	-	-	44.79	-	BL Lac-LSP
2FGL J0012.9-3954	0.27	2010/6/3-2010/6/6	12.66	-0.20	-	-	-	45.73	-	BL Lac-LSP
2FGL J0021.6-2551	0.27	2010/6/15-2010/6/16	14.55	-0.13	-	-	-	45.95	-	BL Lac-ISP
2FGL J0022.5+0607	0.27	2010/6/28-2010/6/29	13.45	-0.14	-	-	-	45.78	-	BL Lac-LSP
2FGL J0029.2-7043	0.27	2010/05/02-2010/05/06	12.33	-0.22	-	-	-	44.96	-	BL Lac-LSP
2FGL J0035.8+5951	0.27	2010/7/10	17.00	-0.11	-	-	-	46.81	-	BL Lac-HSP
2FGL J0038.1+0015	0.7395	2010/6/29-2010/6/30	13.52	-0.17	-	-	-	46.09	-	BL Lac-LSP
2FGL J0045.3+2127	0.27	2009/5/29	15.42	-0.09	-	-	-	46.37	-	BL Lac-HSP
2FGL J0050.2+0234	1.44	2010/7/2-2010/7/6	13.54	-0.15	-	-	-	47.05	-	BL Lac-LSP
2FGL J0050.6-0929	0.635	2009/5/24	15.45	-0.07	-	-	-	47.25	47.29	BL Lac-HSP
2FGL J0057.9-3236	1.37	2009/09/25-2009/09/26	14.31	-0.12	-	-	-	46.30	-	BL Lac-ISP
2FGL J0100.2+0746	0.27	2010/7/9	12.76	-0.24	-	-	-	47.30	-	BL Lac-LSP
2FGL J0100.2+0746	0.27	2010/7/9	12.76	-0.14	-	-	-	45.22	46.47	BL Lac-LSP
2FGL J0114.7+1326	0.27	2010/7/15	15.07	-0.11	-	-	-	46.45	-	BL Lac-LSP
2FGL J0120.4-2700	0.559	2010/1/27	14.44	-0.06	-	-	-	47.55	48.07	BL Lac-HSP
2FGL J0120.4-2700	0.559	2010/1/27	14.44	-0.10	9.54	-	-	47.91	-	BL Lac-ISP
2FGL J0124.5-0621	0.27	2010/7/9-2010/7/10	13.80	-0.15	1	-	-	46.67	-	BL Lac-LSP
2FGL J0136.5+3905	0.27	2010/1/27	16.40	-0.08	-	-	-	45.38	-	BL Lac-LSP
2FGL J0141.5-0928	0.733	2010/5/30-2010/6/6	13.46	-0.17	-	-	-	46.75	-	BL Lac-HSP
2FGL J0144.6+2704	0.27	2010/1/19	13.47	-0.17	9.84	-	-	46.92	47.33	BL Lac-LSP
2FGL J0153.9+0823	0.27	2010/3/1	15.15	-0.10	1	-	-	47.12	-	BL Lac-LSP
2FGL J0203.6+7235	0.27	2010/1/11	-	-0.08	-	-	-	45.82	-	BL Lac-LSP
2FGL J0203.6+7235	0.27	2009/9/11	-	-0.08	-	-	-	46.27	-	BL Lac
2FGL J0204.0+3045	0.761	2010/1/25	12.42	-0.17	-	-	-	45.82	-	BL Lac-LSP
2FGL J0210.7-5102	1.003	2009/11/26	13.30	-0.15	9.8	-	-	46.10	-	BL Lac-LSP
2FGL J0238.7+1637	0.94	2010/1/30	13.09	-0.08	7	-	-	47.32	48.08	BL Lac-LSP
2FGL J0238.7+1637	0.94	2010/1/30	13.09	-0.25	8	-	-	47.99	-	BL Lac-LSP
2FGL J0334.2-4008	1.445	2010/1/17-2010/1/18	13.18	-0.09	4	-	-	47.42	48.31	BL Lac-LSP
2FGL J0334.2-4008	1.445	2010/1/17-2010/1/18	13.18	-0.17	-	-	-	48.25	-	BL Lac-LSP
2FGL J0428.6-3756	1.03	2010/8/17	13.19	-0.06	-	-	-	47.64	48.18	BL Lac-LSP
2FGL J0428.6-3756	1.03	2010/8/17	13.19	-0.20	-	-	-	48.04	-	BL Lac-LSP
2FGL J0516.8-6207	0.27	2009/1/15	-	-	-	-	-	47.54	-	BL Lac-LSP
2FGL J0516.8-6207	0.27	2009/1/15	-	-0.06	-	-	-	46.10	-	BL Lac
2FGL J0523.0-3628	0.055	2010/3/5	13.38	-0.18	8.477	43.38	5	45.32	45.58	BL Lac-LSP
2FGL J0538.8-4405	0.892	2010/3/3	13.74	-0.07	6	9	6	45.24	-	BL Lac-LSP
2FGL J0538.8-4405	0.892	2010/3/3	13.74	-0.14	8.778	45.31	13	48.09	-	BL Lac-LSP
2FGL J0712.9+5032	0.27	2009/1/21	13.72	-	6	9	6	-	-	BL Lac-LSP
2FGL J0712.9+5032	0.27	2009/1/21	13.72	-0.18	-	-	-	46.39	46.59	BL Lac-LSP
2FGL J0721.9+7120	0.27	2005/4/4	14.62	-0.05	-	-	-	46.15	-	BL Lac-LSP
2FGL J0721.9+7120	0.27	2005/4/4	14.62	-0.12	-	-	-	48.29	48.64	BL Lac-ISP
2FGL J0738.0+1742	0.424	2010/10/7	14.04	-0.06	-	-	-	48.38	-	BL Lac-LSP
2FGL J0738.0+1742	0.424	2010/10/7	14.04	-0.16	8.2	-	-	46.57	-	BL Lac-ISP
2FGL J0818.2+4223	0.53	2010/10/15	13.22	-	7	-	-	-	-	BL Lac-LSP
2FGL J0818.2+4223	0.53	2010/10/15	13.22	-0.14	-	-	-	46.46	-	BL Lac-LSP
2FGL J0854.8+2005	0.306	2010/4/10	13.87	-	-	-	-	-	-	BL Lac-LSP
2FGL J0854.8+2005	0.306	2010/4/10	13.87	-0.12	8.79	43.6	14.289	46.64	46.78	BL Lac-LSP
2FGL J0909.2+2308	0.223	2010/5/22-2010/5/26	15.17	-0.18	4	4	4	46.23	-	BL Lac-LSP
2FGL J0909.2+2308	0.223	2010/5/22-2010/5/26	15.17	-0.11	-	-	-	45.31	-	BL Lac-HSP
2FGL J0915.8+2932	0.101	2010/10/28	16.04	-	-	-	-	-	-	BL Lac-HSP
2FGL J0915.8+2932	0.101	2010/10/28	16.04	-0.11	-	-	-	45.27	-	BL Lac-HSP
2FGL J0958.6+6533	0.367	2010/3/12	13.27	-	-	-	-	-	-	BL Lac-LSP
2FGL J0958.6+6533	0.367	2010/3/12	13.27	-0.25	-	-	-	46.59	46.90	BL Lac-LSP
2FGL J0958.6+6533	0.367	2010/3/12	13.27	-0.07	-	-	-	46.60	-	BL Lac-LSP
2FGL J1001.0+2913	0.558	2010/5/7-2010/5/8	13.31	-0.17	-	-	-	46.45	-	BL Lac-LSP
2FGL J1001.0+2913	0.558	2010/5/7-2010/5/8	13.31	-	-	-	-	-	-	BL Lac-LSP
2FGL J1015.1+4925	0.212	2010/4/28-2010/5/1	15.53	-0.13	-	-	-	46.06	-	BL Lac-HSP
2FGL J1015.1+4925	0.212	2010/4/28-2010/5/1	15.53	-	-	-	-	-	-	BL Lac-HSP
2FGL J1043.1+2404	0.559117	2010/7/9	13.28	-0.16	-	-	-	46.48	46.80	BL Lac-LSP
2FGL J1043.1+2404	0.559117	2010/7/9	13.28	-0.07	-	-	-	46.51	-	BL Lac-LSP
2FGL J1057.0-8004	0.581	2010/8/30	12.97	-0.18	-	-	-	46.78	-	BL Lac-LSP
2FGL J1057.0-8004	0.581	2010/8/30	12.97	-	-	-	-	-	-	BL Lac-LSP
2FGL J1058.4+0133	0.888	2009/12/3	13.14	-0.14	7.37	-	14	47.47	47.83	BL Lac-LSP
2FGL J1058.4+0133	0.888	2009/12/3	13.14	-0.04	3	-	3	47.57	-	BL Lac-LSP
2FGL J1058.6+5628	0.14333	2010/4/18-2010/5/4	15.07	-0.15	-	-	-	45.51	-	BL Lac-HSP
2FGL J1058.6+5628	0.14333	2010/4/18-2010/5/4	15.07	-	-	-	-	-	-	BL Lac-HSP
2FGL J1104.4+3812	0.03	2009/11/15-2009/11/17	16.13	-0.13	8.22	41.4	3.3	45.90	45.94	BL Lac-HSP
2FGL J1104.4+3812	0.03	2009/11/15-2009/11/17	16.13	-0.20	4	4	4	44.88	-	BL Lac-HSP
2FGL J1217.8+3006	0.13	2009/12/3-2009/12/19	14.82	-0.10	-	-	-	45.59	45.88	BL Lac-ISP
2FGL J1217.8+3006	0.13	2009/12/3-2009/12/19	14.82	-0.07	-	-	-	45.57	-	BL Lac-ISP
2FGL J1136.7+7009	0.046	2008/10/30	15.68	-0.07	-	-	-	44.61	-	BL Lac-HSP
2FGL J1136.7+7009	0.046	2008/10/30	15.68	-	-	-	-	-	-	BL Lac-HSP
2FGL J1141.9+1550	0.299	2010/6/4-2010/6/8	12.59	-0.27	-	-	-	45.19	-	BL Lac-LSP
2FGL J1141.9+1550	0.299	2010/6/4-2010/6/8	12.59	-	-	-	-	-	-	BL Lac-LSP
2FGL J1146.8-3812	1.048	2010/6/24	12.81	-0.18	8.5	-	13.78	46.97	47.47	BL Lac-LSP
2FGL J1146.8-3812	1.048	2010/6/24	12.81	-0.04	1	-	8	47.30	-	BL Lac-LSP
2FGL J1204.3-0711	0.184	2010/8/9	15.01	-0.17	-	-	-	45.44	-	BL Lac-HSP
2FGL J1204.3-0711	0.184	2010/8/9	15.01	-	-	-	-	-	-	BL Lac-HSP
2FGL J1221.3+3010	0.18365	2010/6/7	16.42	-0.13	-	-	-	45.94	-	BL Lac-HSP
2FGL J1221.3+3010	0.18365	2010/6/7	16.42	-	-	-	-	-	-	BL Lac-HSP
2FGL J1221.4+2814	0.102	2009/12/10-2009/12/12	14.48	-0.15	-	-	-	45.50	45.78	BL Lac-ISP
2FGL J1221.4+2814	0.102	2009/12/10-2009/12/12	14.48	-0.05	-	-	-	45.45	-	BL Lac-ISP

Table 5. Continued.

Fermi name	Z	time	$\text{Log}\nu_{syn}^{peak}$	c_{syn}	$\text{log}M_{BH}$	$\text{log}L_{BLR}$	Γ	$\text{Log}L_{syn}$	$\text{log}L_{bol}$	Blazar type.
(1)	(2)	(3)	(4)	$c_{IC}^{(5)}$	Ref. (6)	Ref. (7)	Ref. (8)	$\text{Log}L_{IC}^{(9)}$	(10)	(11)
2FGLJ1248.2+5820	0.8474	2010/5/20	15.30	-0.16	-	-	-	47.41	47.64	BL Lac-HSP
2FGLJ1427.0+2347	0.16	2010/1/22-2010/1/23	14.94	-0.09	-	-	-	47.26	-	BL Lac-ISP
2FGLJ1428.6+4240	0.129172	2010/6/28	17.68	-0.15	-	-	-	46.14	-	BL Lac-ISP
2FGLJ1428.6+4240	0.129172	2010/6/28	17.68	-0.09	-	-	-	45.48	-	BL Lac-HSP
2FGLJ1442.7+1159	0.16309	2010/2/26-2010/3/9	16.94	-0.09	-	-	-	45.36	-	BL Lac-HSP
2FGLJ1443.9-3908	0.065	2009/9/24	15.80	-0.14	-	-	-	44.99	-	BL Lac-HSP
2FGLJ1517.7-2421	0.048	2010/2/20	13.79	-0.15	-	-	-	44.93	45.20	BL Lac-LSP
2FGLJ1542.9+6129	0.117	2009/1/18-2009/1/20	14.84	-0.03	-	-	-	44.88	-	BL Lac-LSP
2FGLJ1542.9+6129	0.117	2009/1/18-2009/1/20	14.84	-0.11	-	-	-	45.19	45.66	BL Lac-ISP
2FGLJ1653.9+3945	0.033	2010/3/21	16.30	-0.05	-	-	-	45.48	-	BL Lac-LSP
2FGLJ1653.9+3945	0.033	2010/3/21	16.30	-0.07	8.62	41.36	4.2	44.94	45.08	BL Lac-HSP
2FGLJ1719.3+1744	0.137	2009/1/8	13.55	-0.15	4	4	4	44.51	-	BL Lac-LSP
2FGLJ1719.3+1744	0.137	2009/1/8	13.55	-0.14	-	-	-	45.14	46.25	BL Lac-LSP
2FGLJ1728.2+5015	0.055	2010/5/1	16.10	-0.03	-	-	-	46.22	-	BL Lac-HSP
2FGLJ1728.2+5015	0.055	2010/5/1	16.10	-0.13	-	-	-	44.66	-	BL Lac-HSP
2FGLJ1744.1+1934	0.084	2010/3/20-2010/3/27	-	-	-	-	-	-	-	BL Lac
2FGLJ1744.1+1934	0.084	2010/3/20-2010/3/27	-	-0.09	-	-	-	44.54	-	BL Lac
2FGLJ1751.5+0938	0.322	2010/4/1	12.68	-0.21	8.34	-	8.892	46.36	46.70	BL Lac-LSP
2FGLJ1800.5+7829	0.68	2009/10/13	13.88	-0.11	4	-	4	46.43	-	BL Lac-LSP
2FGLJ1800.5+7829	0.68	2009/10/13	13.88	-0.12	7.92	44.56	1.1	47.27	47.65	BL Lac-LSP
2FGLJ1806.7+6948	0.051	2009/11/3-2009/11/5	14.25	-0.06	4	4	4	47.42	-	BL Lac-ISP
2FGLJ1806.7+6948	0.051	2009/11/3-2009/11/5	14.25	-0.08	-	-	-	44.57	-	BL Lac-ISP
2FGLJ2000.0+6509	0.047	2009/9/26	16.43	-	-	-	-	-	-	BL Lac-HSP
2FGLJ2000.0+6509	0.047	2009/9/26	16.43	-0.09	8.09	-	-	45.18	-	BL Lac-HSP
2FGLJ2009.5-4850	0.071	2009/10/5	15.60	-	5	-	-	-	-	BL Lac-HSP
2FGLJ2009.5-4850	0.071	2009/10/5	15.60	-0.09	9.03	-	-	45.65	-	BL Lac-HSP
2FGLJ2022.5+7614	0.594	2010/6/12-2010/6/16	14.41	-	5	-	-	-	-	BL Lac-ISP
2FGLJ2022.5+7614	0.594	2010/6/12-2010/6/16	14.41	-0.08	-	-	-	46.68	-	BL Lac-ISP
2FGLJ2039.1-1046	0.27	2010/4/28-2010/4/29	13.75	-	-	-	-	-	-	BL Lac-LSP
2FGLJ2039.1-1046	0.27	2010/4/28-2010/4/29	13.75	-0.15	-	-	-	46.10	-	BL Lac-LSP
2FGLJ2133.8-0154	1.284	2010/5/16-2010/5/17	13.09	-	-	-	-	-	-	BL Lac-LSP
2FGLJ2133.8-0154	1.284	2010/5/16-2010/5/17	13.09	-0.19	-	-	-	47.55	-	BL Lac-LSP
2FGLJ2152.4+1735	0.871	2010/4/8-2010/4/10	13.70	-	-	-	-	-	-	BL Lac-LSP
2FGLJ2152.4+1735	0.871	2010/4/8-2010/4/10	13.70	-0.15	-	-	-	46.76	47.14	BL Lac-LSP
2FGLJ2158.8-3013	0.116	2010/5/12	15.11	-0.10	-	-	-	46.91	-	BL Lac-HSP
2FGLJ2158.8-3013	0.116	2010/5/12	15.11	-0.16	-	-	-	46.22	-	BL Lac-HSP
2FGLJ2202.8+4216	0.069	2009/12/23-2009/12/26	-	-	-	-	-	-	-	BL Lac
2FGLJ2202.8+4216	0.069	2009/12/23-2009/12/26	-	-	8.23	42.38	6.99842	-	-	BL Lac
2FGLJ2247.2-0002	0.949	2010/1/14-2010/1/16	13.62	-0.10	4	4	4	44.71	-	BL Lac-LSP
2FGLJ2247.2-0002	0.949	2010/1/14-2010/1/16	13.62	-0.15	-	-	-	46.77	47.17	BL Lac-LSP
2FGLJ2258.8-5524	0.479	2010/8/5	15.83	-0.04	-	-	-	46.95	-	BL Lac-HSP
2FGLJ2258.8-5524	0.479	2010/8/5	15.83	-0.16	-	-	-	46.06	-	BL Lac-HSP
2FGLJ2315.7-5014	0.808	2010/5/17-2010/5/18	13.35	-	-	-	-	-	-	BL Lac-LSP
2FGLJ2315.7-5014	0.808	2010/5/17-2010/5/18	13.35	-0.16	-	-	-	46.77	-	BL Lac-LSP
2FGLJ2323.8+4212	0.059	2010/2/20-2010/2/26	15.82	-	-	-	-	-	-	BL Lac-HSP
2FGLJ2323.8+4212	0.059	2010/2/20-2010/2/26	15.82	-0.24	-	-	-	44.45	-	BL Lac-HSP
2FGLJ2330.6-3723	0.27	2010/5/27-2010/6/4	13.59	-	-	-	-	-	-	BL Lac-LSP
2FGLJ2330.6-3723	0.27	2010/5/27-2010/6/4	13.59	-0.14	-	-	-	45.70	-	BL Lac-LSP
2FGLJ2347.0+5142	0.044	2010/1/13-2010/1/22	-	-	-	-	-	-	-	BL Lac
2FGLJ2347.0+5142	0.044	2010/1/13-2010/1/22	-	-	8.8	-	-	-	-	BL Lac
2FGLJ2347.0+5142	0.044	2010/1/13-2010/1/22	-	-0.14	11	-	-	44.00	-	BL Lac

References. 1: Chen et al.(2015); 2: Xiong et al.(2014b); 3: Ghisellini et al.(2014); 4: Chai et al.(2012); 5: Woo & Urry (2002); 6: Ghisellini et al.(2011); 7: Liang & Liu (2003); 8: Xie et al. (2007); 9: Celotti et al.(1997); 10: Shaw et al.(2012); 11: Zhang et al. (2012).